2020

BENEFICIATION OF COAL USING SUPERCRITICAL WATER AND CARBON DIOXIDE EXTRACTION

Matthew DeCuir Virginia Commonwealth University CL
Virginia Commonwealth University

Beneficiation of Coal using Supercritical Water and Carbon Dioxide Extraction

A dissertation submitted in partial fulfillment of the requirements for the degree of Doctor of Philosophy at Virginia Commonwealth University.

By

Matthew J. DeCuir

Bachelor of Science in Chemical Engineering, Auburn University, 2015

Advisor: Ram B. Gupta, Ph.D.

Associate Dean for Faculty Research Development | Professor of Chemical & Life Science Engineering, Department of Chemical & Life Science Engineering

Virginia Commonwealth University
Richmond, Virginia

Defended July 22, 2020

Acknowledgements

This study was supported by the Office of Fossil Energy, U.S. Department of Energy via Leonardo Technologies, Inc., subcontract LTI-F80022594-VCU. Author is thankful to Rosebud Mining Company and Dr. Arif Sikder for providing coal sample and to the dissertation committee for scientific discussions. Thank you to all of graduate students that I have worked with, and especially to my advisor Dr. Gupta.

Table of Contents

List of Figures

List of Tables

List of Abbreviations

$ScCO_2$	Supercritical carbon dioxide
HAP	Hazardous aerosolized pollutants
WFGS	Wet flue gas desulfurization
ScWC	Supercritical water-carbon dioxide
CO_2	Carbon Dioxide
H_2O	Water
CO2	Carbon Dioxide
H2O	Water

Abstract

BENEFICIATION OF COAL USING SUPERCRITICAL WATER AND CARBON DIOXIDE EXTRACTION

by

Matthew J. DeCuir

A dissertation submitted in partial fulfillment of the requirements for the degree of Doctor of Philosophy at Virginia Commonwealth University, 2020

Advisor: Ram B. Gupta, Ph.D.

Associate Dean for Faculty Research Development | Professor of Chemical & Life Science Engineering, Department of Chemical & Life Science Engineering

This work explores the use of carbon dioxide, water, and their mixtures as solvent for the pre-combustion beneficiation of raw coal without using any toxic mineral acids in the temperature range of 200-400°C. The fluid polarity, ionic constant, and supercritical point can be adjusted by H_2O/CO_2 ratio and temperature. Adding carbon dioxide to hydrothermal fluid also increases the ionization by forming carbonic acid. Extractions with supercritical fluids have several benefits including enhanced mass transport, ease of separation and recycle, wide range of extractive capability and tunability, better inherent safety, and in the case of carbon dioxide and water – low cost. A semi-continuous extraction system was designed and built in which pressure, temperature and the relative flow rates of CO_2 and H_2O can be controlled. Coal powder is kept in a packed bed and the extraction is carried out at 143 bar pressure. Using sulfur as a model heteroatom, extractive efficiency is examined as a function of the temperature, fluid composition, fluid flow, and extraction time. Results indicated that carbon dioxide, water, and supercritical water-carbon

dioxide (ScWC) all can effectively extract about 50% of total sulfur from bituminous coal in one hour. Extraction above 350°C decreased effectiveness, and extraction above the supercritical point of pure water caused polymerization presumably due to hydrothermal carbonization. Elimination of organic sulfur may play a role in the polymerization. The carbonized coal that was obtained from extraction above 350°C gives an interesting product that is clean, porous, and partly graphitic in nature. The material could have exciting applications to replace metallurgical coke in metal refining and anode carbon in energy storage applications. Some carbonization occurred in pure carbon dioxide around 350°C as well. Additionally, ScWC extraction may provide necessary control to prevent organic dissolution while removing sulfur. While neither carbon dioxide nor water seemed to affect the ash content, ScWC extraction decreased the ash content to 3.77%, a 45% reduction in ash.

The extraction process was further developed to introduce ultrasound energy to enhance mass transfer from solid coal particles to the fluid phase. At the high temperature and pressure conditions as noted above, the introduction of ultrasound was successful and tested for coal extraction. The degree of mass transfer enhancement can be controlled by the intensity of the ultrasound. Such an enhancement, opens up possibility of relaxing the requirement on the fine particle size of the coal. We found that the conversion of pyrite was nearly complete for the best extracted samples with organic sulfur mostly untouched, indicating that the mass transport even without ultrasound was fairly good.

In the base design of the extractor, the fluid entry and exit points are both on the top cover plate of the vessel. Here scWC fluid enters at the top and then leaves from the top after extraction, so it is possible that not all the coal solids are efficiently contacted with the fresh fluid coming in. To overcome this possible channeling effect, we have further enhanced the extractor design. The

apparatus is designed to allow for the fluid to enter at the top, go through the pack bed of coal, and then exit from the bottom carrying extracted components. The design was tested successfully.

Chapter 1. Introduction

1.1 Coal Use and Industry

Despite recent emergence of natural gas, nuclear, solar, and wind power, coal remains an important energy source to the United States and the world. For example, in 2018, 27.4% of the United States energy demand was met by burning coal, while for the world the number was even higher, about 40%. According to proven reserves, the world has about 150 years' worth of energy from coal combustion, but only 50 years' worth of energy from oil or natural gas. Furthermore, the United States owns 28% of the world's coal reserves compared to only 2.3% of the world's oil reserves. (EIA International Energy Outlook 2017, 2018)

Country	Anthracite and Bituminous	Sub-bituminous	Lignite	Total	% of the World
United States	108,501	98,618	30,176	237,295	22.6
Russia	49,088	97,472	10,450	157,010	14.4
China	62,200	33,700	18,600	114,500	12.6
Australia	37,100	2100	37,200	76,400	8.9
India	56,100	0	4500	60,600	7.0
Germany	99	0	40,600	40,699	4.7
Ukraine	15,351	16,577	1945	33,873	3.9
Kazakhstan	21,500	0	12,100	33,600	3.9
South Africa	30,156	0	0	30,156	3.5
Serbia	9	361	13,400	13,770	1.6
Colombia	6366	380	0	6746	0.8
Canada	3474	872	2236	6528	0.8
Poland	4338	0	1371	5709	0.7
Indonesia	1520	2904	1105	5529	0.6
Brazil	0	4559	0	4559	0.5
Greece	0	0	3020	3020	0.4
Bosnia and Herzegovina	484	0	2369	2853	0.3
Mongolia	1170	0	1350	2520	0.3
Bulgaria	2	190	2174	2366	0.3
Pakistan	0	166	1904	2070	0.3
Turkey	529	0	1814	2343	0.3
Uzbekistan	47	0	1853	1900	0.2
Hungary	13	439	1208	1660	0.2
Thailand	0	0	1239	1239	0.1
Mexico	860	300	51	1211	0.1
Iran	1203	0	0	1203	0.1
Czech Republic	192	0	908	1100	0.1
Kyrgyzstan	0	0	812	812	0.1
Albania	0	0	794	794	0.1
North Korea	300	300	0	600	0.1
New Zealand	33	205	333–7000	571–15,000	0.1
Spain	200	300	30	530	0.1
Laos	4	0	499	503	0.1
Zimbabwe	502	0	0	502	0.1
Argentina	0	0	500	500	0.1
All others	3421	1346	846	5613	0.7
World total	404,762	260,789	195,387	860,938	100

Figure 2: Inventory of the global coal reserves of which 22.6% is in the United States. BP (British Petroleum) Statistical Review of World Energy

Despite this reserve of coal, the production of coal has been decreasing since 2008 due to the rise of natural gas combined cycle generators (Odetayo 2018, De Gouw 2014), fracking (Weinhold, 2012), and concerns over atmospheric and local air pollution (Seinfeld, 2016).

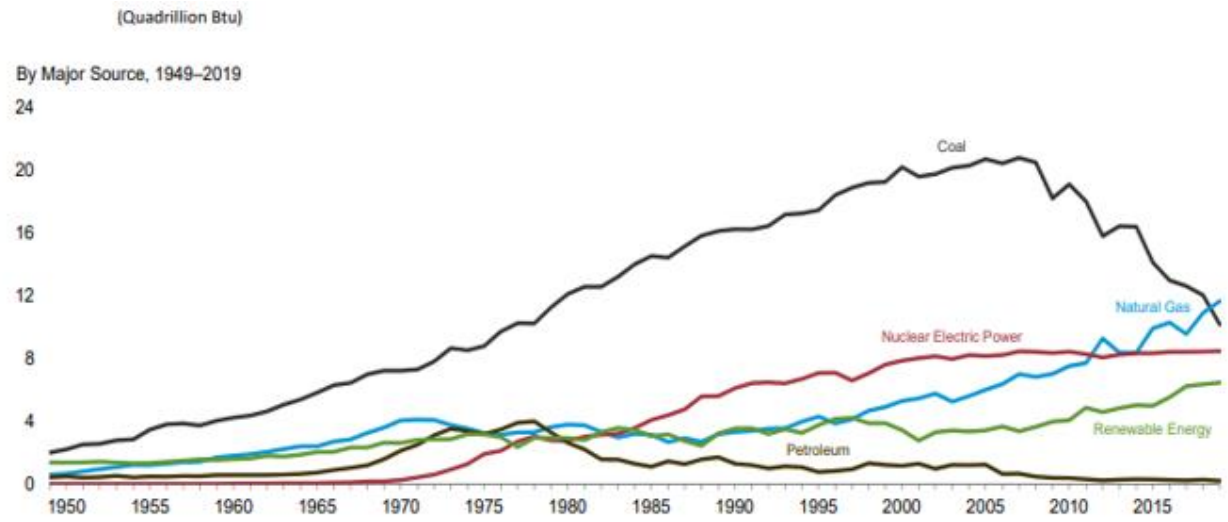

Figure 3: United States contribution to electric power consumption by source. EIA June 2020 Monthly Energy Review

Although coal had dominated U.S. electric power production for many years, natural gas generation has recently overtaken coal based power production. Stringent air quality standards set by the EPA and MATS compliance have placed restrictions on the particulates, sulfur, and NOx emissions of coal fired power plants due to the realization that serious local and global health concerns can arise from their unabated release (Sebor, 2014). Even before decreases in coal fired generation between 2006-2015, sulfur dioxide emissions from coal were decreasing due to an increase in mandates to clean combustion exhaust. Even in 2015 after a 25% reduction in coal fired generation and widespread adoption of exhaust cleaning methods, coal dominated the sulfur dioxide emissions in the U.S. The closure of large capital-intensive coal fired generation systems

was forced by natural gas' boom in production, the ease of handling compared to coal, and the difference in sulfur emissions.

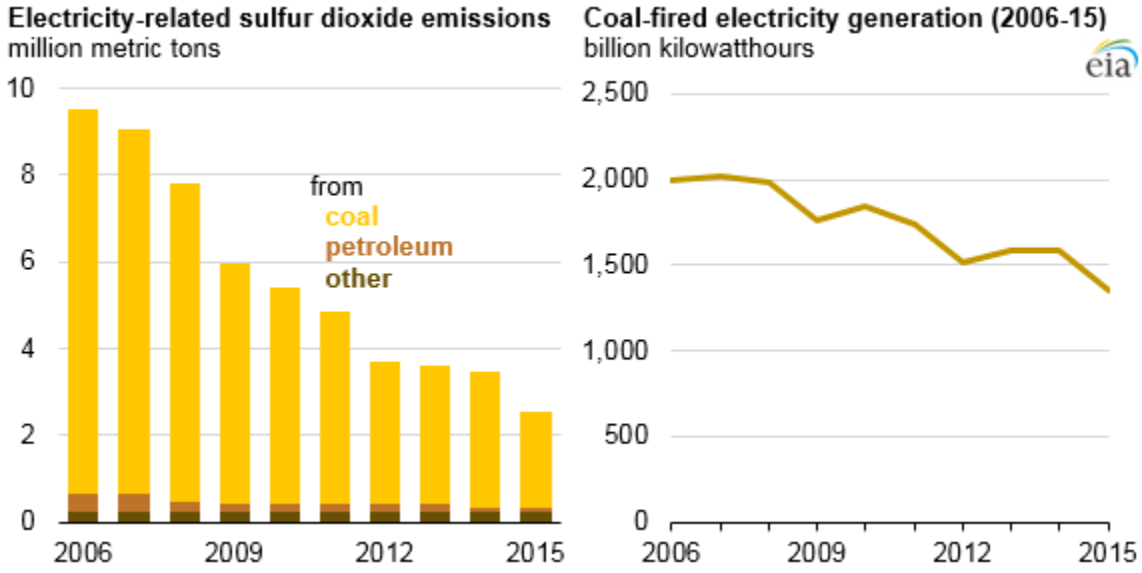

Figure 4: Sulfur Dioxide emissions compared to Coal Fired Generation in the U.S. 2006-2015. U.S. Energy Information Administration, 2018 *Electric Power Annual(released 2019)*

Despite the current energy climate of the U.S. leaning toward natural gas, coal is still the more prominent source for electric power generation around the globe. The petroleum rich Middle East and South and Central America have little coal consumption and can be expected to remain that way. But as Europe and North America decrease their reliance on coal moving forward, the Asian Pacific region has substantially increased coal consumption in the last several decades. Africa may also see a substantial increase in energy consumption in the coming decades that would look similar to the increase in coal consumption in the Asia Pacific due to the wealth of coal in Africa (Pollet 2015).

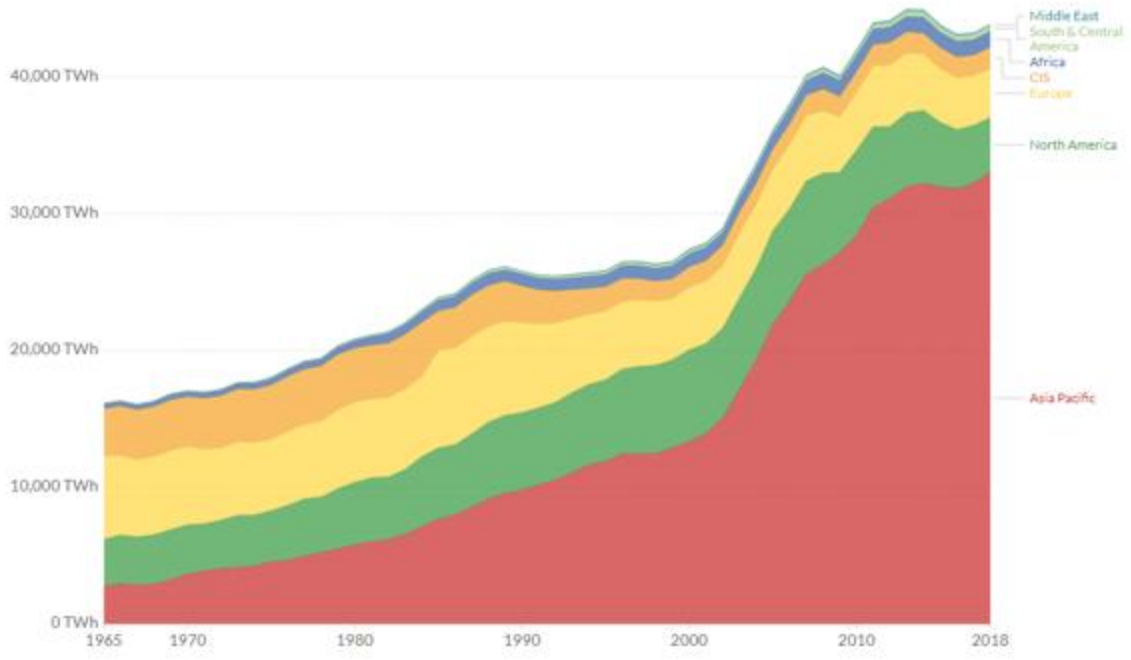

Figure 5. Rise in the global coal consumption over the last five decades (2019 BP Statistical Review)

Liquid and solid hydrocarbons are both finite resources that will deplete in time. Solid hydrocarbon coals are sourced from decayed and compacted plant matter, as opposed to petroleum and natural gas which are the product of compacted animal remains (Teichmüller 1966). While eons of crustaceans may contribute to substantial liquid hydrocarbon reserves in the oceans, the surface has been more heavily populated with flora and thus coals. Another 100 years may pass before liquid hydrocarbons become hard to find, but coal should be around for another half millennium. With the world's population trending ever higher, all sources of energy are important now and into the future because access to energy is so closely tied to quality of life.

1.2 Coal Structure and Chemistry

Raw coal is ranked by its carbon content into four major categories – peat, lignite, bituminous coal, and anthracite. Peat and lignite are low rank coals which have not been exposed to enough pressure for enough time to develop into higher rank coals. Bituminous coals are the most commonly used coals for large scale electric production, but lignite is also popular. Anthracite is the highest rank coal and is often very dense. The moisture, volatile matter, and oxygen content of coal decrease with rank, and the carbon content increases with rank.

Coalification stage	Moisture[a] (%)	Volatile matter[b] (%)	Carbon content[b] (%)	Calorific value[a] (kcal/kg)	Oxygen content[b] (%)
Peat	~75	69–63	< 60	3500	> 23
Lignite	35–55	63–53	65–70	4000–4200	23
Sub-bituminous C	30–38	53–50	70–72	4200–4600	20
Sub-bituminous B	25–30	50–46	72–74	4600–5000	18
Sub-bituminous A	18–25	46–42	74–76	5000–5500	16
High volatile bituminous C	12–18	46–42	76–78	5500–5900	12
High volatile bituminous B	10–12	42–38	78–80	5900–6300	10
High volatile bituminous A	8–10	38–31	80–82	6300–7000	8
Medium volatile bituminous	8–10	31–22	82–86	7000–8000	4
Low volatile	8–10	22–14	86–90	8000–8600	3
Semi-Anthracite	8–10	14–8	90	7800–8000	3.5
Anthracite	7–9	8–3	92	7600–7800	4.5
Meta-Anthracite	7–9	8–3	> 92	7600	5

[a] As received basis.
[b] Dry ash free basis.

Figure 6: Coal Rank (Meshram 2015)

Coal also contains ash and hazardous aerosolized pollutants. Generally higher rank coals contain less ash and sulfur, but mines and regions may vary greatly in ash content and sulfur

compared to others. While North American coals are usually fairly clean and of high rank, Chinese coals are often high in ash content (Yan 2003, He 2016), and Indian coals are known for high sulfur content (Ken 2019, Baruah 2007, Chabukdhara 2016). The ash contains metals and metal oxides ranging from the lightest metals to the heaviest. The most common elements by mass are magnesium, sodium, aluminum, silicon, iron, and calcium (Gabler 1982). Heavy elements are present in ppm concentrations (Qian 2008). When combusted, the lighter ash metals will be swept up with the flue gas and the heavier metals will form slag that impedes unit operations (Baruah 2010). Although some heavy metals are scarce and production is limited to China, light and heavy ash has been collected for centuries and stored in landfills due to the levels of toxic metals that cannot be separated economically from the valuable metals (Humphries 2010, Dai 2016, Lin 2017).

As opposed to the ash content that remains as a solid after combustion, more volatile elements will form noxious vapors that are harder to contain and destructive to the environment. Sulfur, mercury, and chlorine are elements which form hazardous aerosolized pollutants. While mercury and chlorine are often present at ppm levels, sulfur is often present at concentrations of 1-5 mass%. Sulfur in raw coal is present in three forms – pyrite, sulfate, and organic (Calkins 1994). Pyritic sulfur is sulfur that is bound to iron, either as FeS or FeS_2. Sulfate form is not commonly found in nature, but can be formed upon oxidative processing. For the organic form, sulfur can be bonded to the carbon structure in a variety of ways (Davidson 1994). Organic sulfur is found in coal as mercaptans (RSH), disulfides (RS-S-R'), sulfides (R-S-R'), and thiophenes (heterocyclic). Organic sulfur is thus integrated into the carbon structure and difficult to remove. Generally, raw coals may contain a similar amount of sulfur in pyrite and organic forms. Upon combustion, the sulfur in raw coal will form sulfur dioxide, which is toxic to humans if released

to the atmosphere and corrosive to plant equipment. Emission of other highly active molecules, such as chlorine and mercury, also contributes to deterioration of the atmospheric environment (Akers 1996, Yan 2002). Other forms of sulfur possible in less oxidative conditions include hydrogen sulfide and elemental sulfur.

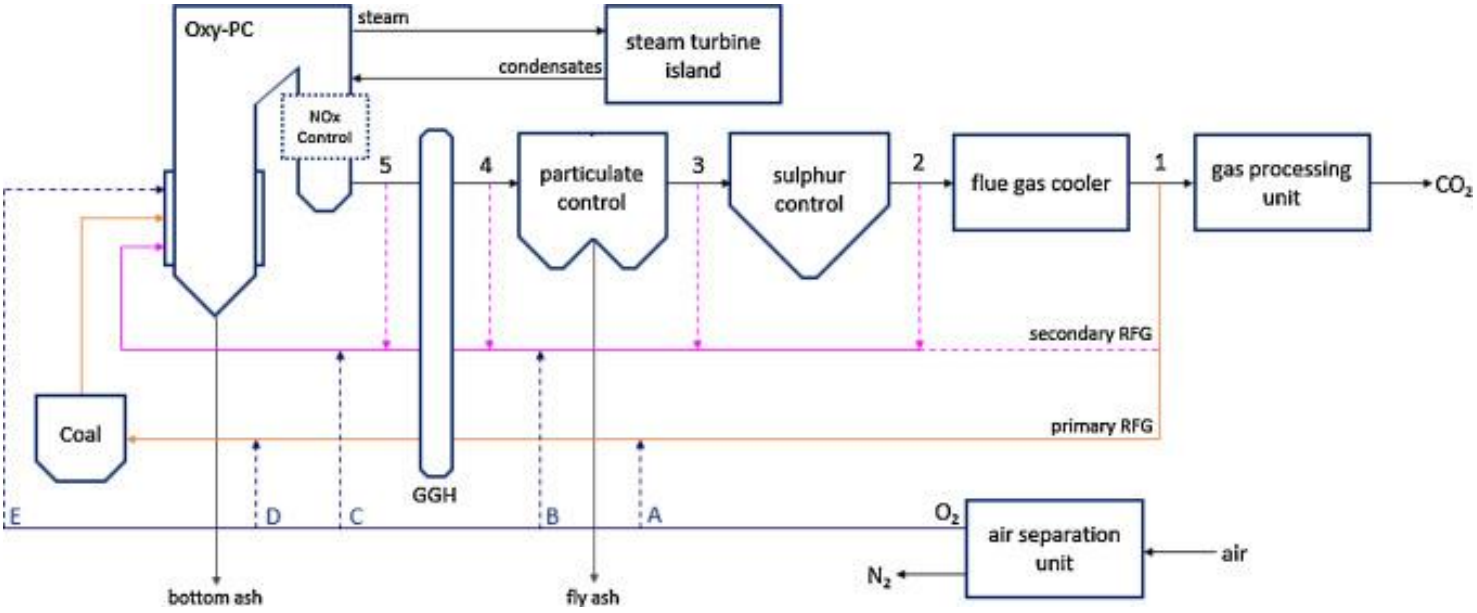

Figure 7: Process schematic for combustion of a low-grade coal. (Fleig 2011)

Figure 6 demonstrates a modern coal fired combustion scheme. Particulate matter from ash combustion is separated from flue gas using electrostatic filters (Wang 2008). Limiting NOx production is achieved by looping of reaction gases and effective flame control (Belošević 2017). Wet flue gas desulphurization (WFGD) units have become the industry standard to limit the sulfur dioxide emissions, with state of the art installations capturing 90-95% of sulfur and a variable amount of chlorine and mercury (Scala 2008, Van Otten 2011). In WFGD, flue gas is passed through concentrated aqueous lime solutions that adsorb SOx vapors. The resultant slurry can be

used to form calcium sulfate dehydrate (i.e., gypsum) but will mostly accumulate as solid waste as elemental sulfur or calcium sulfate. Separating particulates and sulfur from flue gas requires the processing of large volumes of flue gas and leads to a significant thermal load on the plants (Wei 2017). Treatment of waste in air, water, and solids is a concerning issue that has large impacts and costs that are hard to calculate. Improper solid and liquid waste management can lead to failures in the short term requiring remediation efforts (Rivera 2017, Santamarina 2019), but continued air pollution has become a top international concern for the long term (Gupta 2010). The future of allowable and untaxable air pollution is unclear. Thus, current combustion of raw coal leads to a plethora of issues concerning environmental safety, materials handling, and combustion efficiency.

1.3 Pre-combustion extractions

Pre-combustion extractions of raw coal have been an intensive area of research for some time with a few promising methods for removing all of the sulfur and ash content reported recently. Results are summarized in Table 1. The most effective precombustion cleaning methods are classified as biological, physical, or chemical. For biologic coal beneficiation, a bacteria that consumes sulfur at a high rate is allowed to digest the coal. The most effective biologic digestion was shown to remove 72% of the total sulfur content using *Bascillus Subtilis* (El-Midany et al., 2018). Unfortunately, the beneficiation using microbes is slow, costly, and difficult to maintain or scale up.

Physical methods include gravity separation, froth flotation, oil agglomeration, and magnetic separation. In these techniques, a difference in the physical characteristics between mineral matter and coal matter is exploited. In gravity separation, small cyclones enhance the

gravity field in an aqueous medium, forcing light hydrophobic coal particles to the top and causing mineral matter to sink. Gravity separation is more effective at cleaning coarse coals, but is ineffective at removing finely assimilated pyrite. Froth flotation takes advantage of the differences in buoyancy as well, but instead uses surfactants to increase removal efficiency. Oil agglomeration techniques operate very similarly, but use vegetable oils as medium instead of water. Magnetic separation relies on the fact that coal matter is a weakly diamagnetic, but the sulfur and ash components are paramagnetic and iron is strongly paramagnetic. In pilot scale tests, magnetic separation was shown to achieve 40 wt.% total sulfur removal (80 wt.% pyrite removed) and 35 wt.% ash removal (Uslu et al., 2004). While physical remediation of coal is not suitable for chemically bonded minerals and requires energy intensive grinding, industrial implementations of physical coal cleaning methods can be found because of their ease of scalability.

Table 1: Current coal beneficiation to remove sulfur.

Study	**Extraction Method**	**Coal (g)**	**Water (g)**	**Temperature (°C)**	**Sulphur removal (total%)**
Uslu et al., 2004	Magnetic Physical		-	MW heating	55% of pyritic
El-Midany et al., 2014	Bascillus Subtilis	0.1	100	25	72%
Mketo et al., 2016	3M HNO_3-H_2O_2	0.1	12	180 (MW heating)	102%

Saikia et al., 2014	NaOH-KOH with sonication	20	100	25	< 50%
Ambedkar et al., 2011	2 N HNO_3+ 3 vol% H_2O_2 with sonication	20	500	25	41%
Vasilakos et al.,1983	Chlorinated Water	20	350	< 100	70%
Balaz et al., 2001	5% NaOH	20	200	90	42%
Timpe et al., 2001	Hydrothermal	40	10-300 g/min	370	50%

Chemical beneficiation of raw coal is considered the most promising method to effectively remove all sulfur forms. Acids and alkaline solutions can be used sequentially and in various mixtures to produce coal with both low ash and low sulfur. Some commercial ash-free coal methods requiring heated oil as solvent may exist, but the process is not economically feasible. Most of these extraction schemes are inspired from high-value materials; unfortunately, coal is a low value commodity and these methods which call for even dilute acids and microwave radiation cannot be performed economically on an industrial scale. In addition, the residual acids and caustics in the coal, even in small amounts, will be combusted upon use, which creates new environmental challenges. Furthermore, the hydrocarbon bonds should not be broken down so as to retain heating value. While hydrothermal extractions have been used to clean coal, they usually decrease the heating value by a considerable amount due to organic dissolution and fractionation

into gas and liquid phase (Timpe et al. 2001). Recently, a research group did show that carbonic acid could be used to enhance aqueous extraction of coal by bubbling CO_2 through stagnant hot water, but the experimental temperatures and pressures were very mild (Gao et al. 2017; Ding et al. 2019).

1.4 Two-stage, Acid-Base Leaching

The vast majority of efforts on coal beneficiation has been with harsh acid leaching. Typically, harsh acids are employed as the inorganic content is finely distributed in the coal and is difficult to remove. Various extraction sequences and mixtures have been tested over time with full extraction of sulfur only recently reported. For example, Mketo et al. tested several combinations of extracting acids at 180 ^oC for 5 minutes in microwave and found that a mixture of 3 M H_2O_2 and 3 M HNO_3 was able to completely remove sulfur. Other acids tested included HCl and aqua regia, but they drastically reduced the carbon content. A wide range of elements were extracted including Be, Cd, Ce, Co, Cr, Cu, La, Mn, Ni, Pb, Sc, Sm, Sr, Th, V, Y, Zn. Carbon attack for the optimal solution, 3M each peroxide and HNO_3, resulted in decrease of carbon content from 45wt% to 37.7wt%. (Mketo et al., 2016)

Vasilakos et all showed in 1983 that pyrite portions of coal can be extracted with chlorinated water at room temperature. They also tested the effect of various solvents other than water and found that extracting in carbon tetrachloride prevented loss of thermal value of coal seen with water as solvent. (Vasilakos et al., 1983)

In 2000, Balaz reported reducing total sulfur content of coal from 1.9wt% to 1.1 wt% by treating 20 grams coal with 200 mL of 5% NaOH at 90C for 30-120 minutes. Arsenic level was also decreased by 95%.(Baláž et al., 2001).

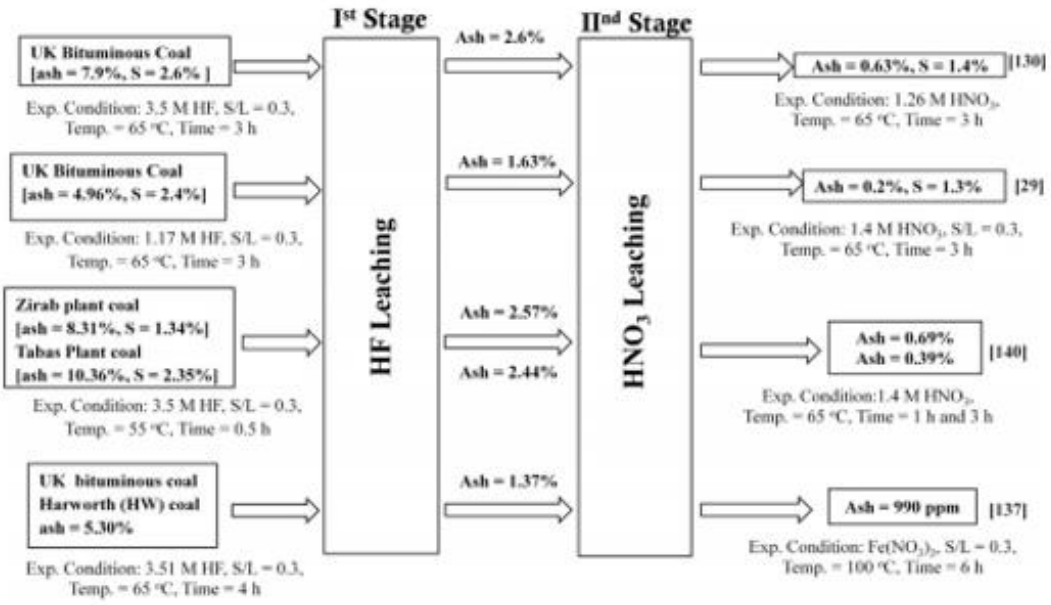

Figure 7. A review of two-stage acid-base demineralization of coal. (Meshram, 2015)

1.5 Thermal Treatment

While thermal treatment in oxygen atmosphere will lead to combustion, thermal treatment in inert atmosphere such as nitrogen has been studied in efforts to liquify and gasify coal. Pressurized CO_2 atmosphere is more oxidative than nitrogen atmosphere, but much less oxidative than oxygen or air atmosphere. While coal behavior in high temperature CO_2 in unknown, studies of combustion, gasification/liquefaction, oxyfuel combustion, and pyrolysis can give some understanding of the coal's carbon and ash behavior and separation in high temperature oxidative environments.

Traditionally, the only pre-combustion extraction performed on coal at a large scale is the production of coke to produce iron. Coke is an upgraded form of coal that has had sulfur, ash, and volatile matter removed by baking in a coke oven in the absence of oxygen at temperatures up to 800°C. Although this process is not economical for power production, the production of steel in a blast furnace requires a solid fuel source that will burn at the correct temperature, usually about

1250 ℃, and add little impurity to the steel. Thus coal is stripped of ash and sulfur using high temperature and then allowed to carbonize to achieve the correct thermal character. Carbonization of coal to coke may take up to 48 hours. Coke and iron ore are packed into a blast furnace. The blast furnace continually consumes ore and coke mix fed from the top and collects liquid steel at the bottom. The industrial operation of coke ovens and blast furnaces are known to be highly toxic to workers as the oven is not a sealed, pressurized vessel, but rather an oven made of brick with leaks.

Further upgrading of coal into carbon materials can be achieved with an Acheson furnace to produce synthetic graphite for carbon filters and battery electrodes on up to high quality graphite. Coke is usually produced by the consumers, but price is generally $300-$500/tonne. Amorphous carbon may cost up to $1000/tonne, and high grade graphite may cost up to $10,000/tonne. Natural graphite is mined, and usually costs about 1/3 the price of synthetic graphite. Natural and synthetic graphite compete, with synthetic carbon chosen by the producers of specialty products and natural graphite chosen by price driven industries.

Coal gasification is the other industrial extraction method for coal. Large scale production of 'town gas' is reported in Germany as early as the mid 1800's using biomass gasification. In gasification schemes, the feedstock is converted at 1200-1600℃ at pressure of 2-8MPa in an atmosphere at promotes the production of syngas. Being above the ash fusion temperature, the molten ash will drain down the walls of the reactor. The syngas must be cooled and treated. Thus, the ash and sulfur are separated by volatilizing the carbon content in a hot, non-combustion step. The process is not energy efficient or economic, but can create clean easily handled fuel.

Qi et al. studied the effect of atmosphere and temperature on coal pyrolysis in the range of 500-900 ^{o}C. They found that the sulfur removal efficiency steadily increases up to 900 ^{o}C. In the

range, 350-455 ^{o}C pyritic sulfur decomposes as well volatilization of organic sulfur. It was also found that increasing temperature in this range resulted in non-organic sulfur being absorbed by the remaining char. This study, most importantly, demonstrated the importance of the oxidative balance of the atmosphere during extraction. For example, adding 0.6% oxygen by volume to nitrogen significantly improved the breaking of organic sulfur bonds above 700 ^{o}C. This group also later found that adding 10 wt% potassium hydroxide would increase desulfurization at 600 ^{o}C from 40-50% to 70-80% (Qi et al., 2004).

Iron, sodium, and potassium shown to have little effect on char gasification. Calcium though catalyzes the gasification reaction by attracting H_2O and CO_2 to the coal surface to react with carbon more easily. Synergistic effect of H_2O with CO_2 was demonstrated for chars gasification at 800 ^{o}C. (Wang et al., 2016).

In 2018, Liu et al. reported on supercritical CO_2 extraction using ethanol at 350 ^{o}C in order to liquify coal into tars rich in phenol, aliphatic esters, methylene. Yield was about 34% by weight when using CO_2 with ethanol as compared to 28.4% for pure ethanol extraction. Coal liquefaction generally takes place at 450 ^{o}C with hydrogen in solvents such as tetralin or 9,10-dihydroanthracene. Typically, 5g coal in 50 mL ethanol with CO_2 pressure of 500 psi, then the vessel heated to temperature, 0.5 hours or 3 hours. N-Heptane was used for the tar filtration and extraction. (Liu et al., 2018)

1.6 Hydrothermal Leaching

While washing coal with water at room temperature is not effective due to its hydrophobic carbon structure, treating the coal with pressurized and superheated water can effectively remove coal substituents.

Timpe et al. hydrothermally treated coal to remove organic sulfur at 370 ^{o}C and 2000-3300 psi pressure. The remove sulfur, the temperature needed to be above 250 ^{o}C and the pressure from 2000 3300 did not have any influence. Organic sulfur and hazardous air pollutants (HAPs: Mercury, Chlorine, Selenium, Arsenic) were reduced by 50%. Sulfur content in the extracted coal remained above 1 wt%. (Timpe et al., 2001)

Bo et al. tested medical waste incinerator fly ash and showed that supercritical water can remove heavy metals such as Cu, Pb, Ba, Cr, Zn, Cd, and As. Typical extraction used 3 g ash in 90 mL water or water and hydrogen peroxide and lasted for 1-4 hours at 425 ^{o}C and 32-42 MPa. Extraction was effective enough to meet us and Chinese EPA limits. (Bo et al., 2009)

1.7 Hydrothermal Carbonization

Hydrothermal treatment is also used to convert low grade biomass such as cellulose, wood, and even sewage with temperatures in the range of 180-220 ℃. The major processes are dehydration and decarboxylation resulting in an increase in carbon content and calorific value. Additionally, the carbonized biomass has lower hydrogen and oxygen content resulting in something close to a low rank coal. Polymerization of the biomass can be explained by the elimination of carboxyl and hydroxyl groups creating unsaturated hydrocarbons which polymerize through stepwise aldol condensation (Kabyemela, Nelson).

Feed	Temperature [°C]	Residence Time [h]	Coal Yield [%]	H/C [-]	O/C [-]
Cellulose				1.67	0.83
	225	3	63	1.29	0.61
	200	50	49	0.76	0.28
Peat Bog				1.34	0.65
	200	10	45	1.00	0.29
	250	0.3	36	0.87	0.23
Wood				1.43	0.58
	200	72	66	0.97	0.25
	250	72	56	0.90	0.17

Figure 8: Hydrothermal Carbonization of biomass. (Funke)

1.8 Ultrasound Treatment

Ultrasound waves can be added to solution to enhance the mass transport of the fluid. A piezoelectric crystal is attached to a horn that is placed in the vessel near the solids. Crystals may also by placed on the exterior of vessels after some calculation, but thick steel will dampen ultrasound waves. Traditionally, the formation of bubbles leads to increased mixing and increased ion activity caused by the collapse of the bubbles. In supercritical solution though, two phases cannot exist and bubbles will not form. Still, the addition of pulsed ultrasound waves are expected to further increase the mixing and mass transport of the supercritical fluid which may be important for penetrating the solid matrix of coal. Most ultrasound studies focus on the use of basic hydroxide solutions that enhance the formation of hydrogen peroxide, which performs the critical steps in chemical extraction of sulfur and ash.

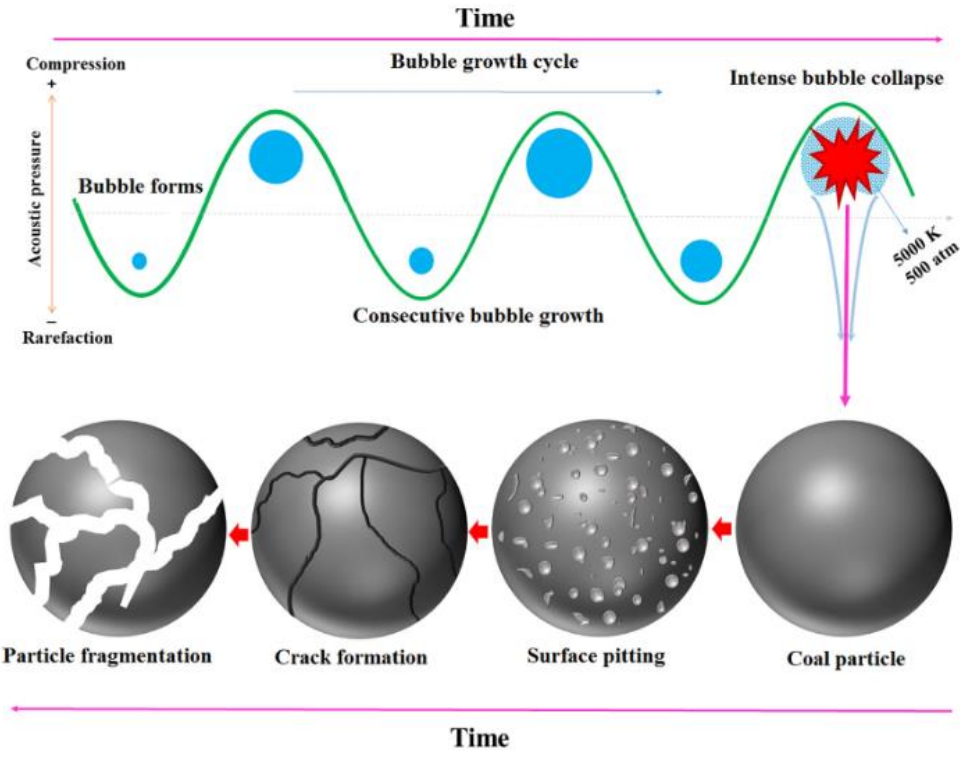

Figure 8: Bubble formation and collapse caused by ultrasound waves. (Barma, 2019)

Saikia et al. tested alkali mixture of 1M:1M KOH and NaOH with 20 kHz ultrasonic energy for 3 hours and found that the ash content and pyritic content was decreased up to 85% but were less effective at removing sulphate or total sulfur (~15%). Effect of ultrasonication on leaching is not well understood. Ultrasound cause mechanical vibrations resulting in cavitation with increased chemical reactivity. In addition, shearing can crack the surface and increase the liquid uptake in the solid matrix by capillary action. The applied ultrasound energy was not enough to break the carbon-sulfur bonds, but that the highly reactive species created by ultrasound in water such as OH radicals, H_2O_2, and ozone oxidize sulfur compounds to sulphoxides, sulphones, and sulphates. (Saikia et al., 2014)

Ambedkar et al. also examined the acid demineralization of coal using ultrasonication. They utilized 2 N HNO_3 with 3 vol% H_2O_2 with 20 kHz sonication at 500W for 30 minutes and

observed 87% sulfur removal. It was concluded that particle breakage due to cavitation is dominant in low-frequency ultrasound, whereas streaming phenomenon is dominant in high-frequency ultrasound. Sonication increases the sulfur removal. (Ambedkar et al., 2011)

1.9 Carbonic Acid Extraction

There are a very few published studies of carbonic acid extraction of coal. Carbonic acid is formed by the dissolution of carbon dioxide in water. H_2CO_3 can donate two hydrogen ions to replace metal ions in the coal structure. Little thermodynamic data exists for carbon dioxide/water ionization at high temperatures or pressures. Recent investigations suggest that the traditionally weak carbonic acid (pH ~5.6) at low temperature and pressure is actually stabilized by high temperature and pressure (pH estimated ~3.2) [1-4].

In 1987, Slegeir first suggested use of carbon dioxide and water as a treatment for coal. They treated batches of coal-water slurry pressurized to 800-1200 psi with CO_2 at 30-80°C, and found that the treatment produced coal with decrease in moisture and ash content and increase in grindability. (reference not found)

In 1989, Otaka et al. treated several coals with CO_2 and found that Ca and Mg contained as carbonate and sulfate minerals were removed easily, but the calcium bound to carboxyl groups was difficult to remove. (reference not found).

In 1991, Hayashi et al. showed that after 12 hours of treatment with 600 kPa carbon dioxide, coal in a water slurry was extracted of calcium and magnesium at levels similar to a wash with hydrochloric acid in which 90% was removed within 30 minutes. Typical coal slurry contained 0.1-3.0 grams coal and 30 grams water. (Hayashi et al., 1991)

In 2005 Masaki et al. reported a pretreatment method for coal extraction of placing coal and water in an autoclave and pressurizing the cell with carbon dioxide. At CO_2 partial pressures of 0.1, 0.5, 1.0, and 7.0 MPa the pH was estimated to be 3.75, 3.52, 3.38, and 3.12, respectively. Subsequent thermal extraction with 0.1 mL/min crude derived organic solvents (not specified) was carried out under 1.0 MPa nitrogen atmosphere and 320-400 ^{o}C to produce ash-free coal (HyperCoal). It was shown that the pretreatment in CO_2 atmosphere increased the hypercoal extraction yield ~10% by increasing removal of calcium and magnesium.(Masaki et al., 2005)

In 2017 and 2019, Gao et al. used low-pressure carbonic acid solutions to leach coal. In a typical experiment, 1 gram of coal slurry suspended in 50 grams of water was bubbled by 200 mL/min CO_2 for 24 hours. The pH was measured to be 5.6. The CO_2 bubbling allowed for the removal of organic forms of sodium and calcium that were not accessible by leaching in water alone. They were able to remove up to 31 wt% of calcium and 71 wt% of sodium. The removal of total ash was found to be 9.4-19.2%. Small differences in efficiency were observed at 25, 40, and 60 ℃; with 60℃ giving the better efficiency. (Gao et al., 2017; Ding et al., 2019)

In 2006, Iwai et al. reported on upgrading low rank coal with supercritical carbon dioxide at 15 MPa and 40 ^{o}C to remove iron and calcium. Experimenting with chelating agents methanol, ethanol, and acetyl acetone they found that recovery rate of iron and calcium were not high but that the acetyl acetone increased recovery rate of iron substantiatally because the acetyl acetone solution had water in it. They remarked that water played a critical role in their extraction. Good recovery rates for calcium were only achieved by adding acetic acid with ethanol to the sCO_2. Recovery was shown to increase with increasing carbon dioxide flowrate and decreasing particle size. (Iwai et al., 2006)

In 2006, Anitescu reviewed the many extractions attempted on soil samples including supercritical water treatment and supercritical carbon dioxide in order to remove organic toxins PCB and PAH. They found that raising the temperature of water to 400 ^{o}C decreased the polarity of water such that extractions were effective. Also, scCO_2 extractions were found to increase in effectiveness by raising the temperature to 200 ^{o}C. (Anitescu et al., 2006)

Although carbonic acid was shown to be effective by several groups at removing lighter metals from coal such as Na, Mg, and Ca for prevention of slagging. Most other ash content was not accessible at the experimental temperatures and pressures used so far. Also, various groups have demonstrated that water enhances supercritical carbon dioxide extractions. Increasing temperature to extract with supercritical water (hydrothermal leaching) has also been shown to be effective, but extractions using heat, water, and pressurized CO_2 all together are experimentally difficult and have not been reported so far. In this work, we would like to examine if combining the three would allow for the extractive conditions to be strong enough to remove higher metals such as iron and sulfur, but weak enough to leave the carbon in the solid form.

The key hypothesis of this work is that by utilizing mixtures of supercritical CO_2 and H_2O at high temperature and pressure conditions, inorganic elements can be selectively extracted from coal. The CO_2-H_2O ratio can be used to fine-tune the extraction efficiency. Ionization provided by the formed carbonic acid along with the high thermal energy can cause reaction of the inorganic content, and the products are then solubilized and efficiently carried away by the high density of the fluid. We are interested in exploring the extraction in the range of 200 – 400 ^{o}C with pressure in the range of 2000-3000 psi which has not been studied before.

1.10 Key Motivation for This Work

Inspired by previous successful extraction efforts but keeping in mind the necessary thermo-economic restrictions for scale up on coal, we propose an extraction using supercritical mixtures of water and carbon dioxide. The mixture will form in-situ carbonic acid capable of leaching heteroatoms from coal but also will be finely tunable to prevent loss of hydrocarbon heating value. Also, supercritical extractions have the benefit of simple separation upon completion of extraction using fractionation at decreasing pressures. Power plants would be able to use carbon dioxide generated from combustion, otherwise emitted, and use waste heat to perform economical and environmentally protective extractions on raw coal. Because sulfur comprises the majority of hazardous aerosolized pollutants by mass, sulfur is studied as a model heteroatom before and after extraction in this work.

1.11 Mechanism of Extraction

Extractions involve the separation of components. Chemical reactions between solvent and extraction target assist in separating the target by forming intermediate complexes that are more soluble in the solvent. The solvent flow also aids in then physically separating the target molecule from its previous bond into the fluid bulk. The three major groups of extractions are cation exchangers, solvating extractants, and anion exchangers. Cation exchangers can be either acidic extractants or chelating extractants. Organic acids such as sulfonic, carboxylic, phosphoric, and phosphonic acid are acid cation exchanging extractants (Qiu 1993). Acid cation exchange is highly pH dependent. Chelating extractants, such as hydroxyoximes, contain two functional groups that form bidenate complexes with metal ions and are used industrially for copped extraction (Flett 1979). Solvating extractions contain electron rich oxygen or sulfur atoms that can bind to metal atoms, forming an anionic coordinating ligand (Mooiman 1991). This extraction relies on the

formation of an uncharged ion pair or complex in the aqueous phase. Examples of solvating extractants are phosphoric esters, alkyl sulfides, and ketones. Anion exchangers such, as quaternary ammonium salts and ranges of amines, are useful for separating metals present in electrolytic solutions as neutral ion pairs or anionic species (IDE 1985).

Also important to extraction is the physical separation caused by the force of the solvent. Pressure washing is a form of extraction where a target, usually dirt, is separated from a sturdier substrate, like driveways or the sides of a building. With pressurized solutions, a similar effect is created when the pressure is decreased and a sharp flow of solvent toward the outlet is created. This phenomenon is referred to as instant controlled pressure drop (DIC) extraction (Allaf 2013, Berka-Zougali 2010).

For large scale use, the extraction must a few simple but difficult to satisfy requirements. First, the solvent mixture must function efficiently in terms of economic constraint. In other words, the cost of the extractant solution cannot exceed the value added to the mass treated. The extracting solvent should be cheap, and the value added to the solid substantial. Second, the solvent must be regenerated in a stripping reaction at a high rate. The solvent should not bond so tightly to the target that the target cannot be removed at some other physical condition allowing for solvent regeneration. Also, the solvent should not attack the substrate so violently that it bonds irreversibly to the substrate, and sent for combustion in the case of coal. Third, the extraction should provide maximum safety to plant personnel and equipment. The inherent danger of handling more caustic and harsh extracting solutions at high flowrates and enthalpy may very easily be preventative to scaleup.

1.12 Supercritical Fluid Extraction

Supercritical fluid extractions have several benefits including enhanced mass transport, ease of separation and recycle, wide range of extractive capability and tunability, and better inherent safety. A fluid is supercritical when it is compressed beyond its critical pressure and heated beyond its critical temperature, and the fluid density can be adjusted by changing pressure and temperature. The diffusivity of the supercritical fluids is higher than that of liquid solvents, and can be easily varied. For typical conditions, diffusivity in supercritical fluids is of the order of 10^{-3} cm^2/s as compared to 10^{-1} for gases and 10^{-5} for liquids. The viscosity of typical supercritical fluids is of the order of 10^{-4} g/cm-s which is similar to that of gases and about 100 fold lower than that of liquids. The combination of the high diffusivity and low viscosity provide rapid equilibration of the fluid to the mixture to be extracted, hence extraction can be reached close to the thermodynamic limits. In addition, the supercritical temperature can be manipulated by changing the pressure, which can be done to ensure that the fluid mix is supercritical at the intended extraction temperature.

For many extraction applications in food and pharmaceutical industries, carbon dioxide is the supercritical fluid of choice because it is non-flammable, non-toxic, inexpensive, and has mild critical temperature (31.1 ^oC and 74 bar). Hence, much of the attention has been given to supercritical carbon dioxide for practical extraction applications. However, $scCO_2$ is too mild for extraction of hard minerals from materials such as coal.

One the other hand, water is supercritical at >374 °C temperature and >221 bar pressure. Supercritical water has liquid-like density and gas-like transport properties, and behaves very differently than it does at room temperature. For example, it is highly non-polar, permitting complete solubilization of the most organic compounds and gases. The resulting single-phase mixture does not have many of the conventional transport limitations that are encountered in multi-

phase reactors. The physiochemical properties of water, such as viscosity, ion product, density, and heat capacity, also change dramatically in the supercritical region with only a small change in the temperature or pressure, resulting in a substantial increase in the rates of chemical reactions (Gupta 2005). For example, Figure 1 shows how density, dielectric constant and ionic product of water vary with temperature at 240 bar.

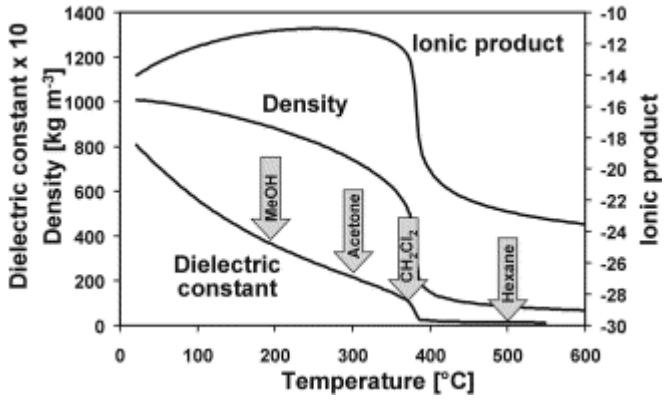

Figure 10. Physical properties of water versus temperature, at 240 bar. Dielectric constants of typical organic solvents at room temperature are also indicated (Kritzer et al. 2001).

From Figure 10, it is interesting to see that the dielectric behavior of 200 ^{o}C water is similar to that of ambient methanol, 300 ^{o}C water is similar to ambient acetone, 370 ^{o}C water is similar to methylene chloride, and 500 ^{o}C water is similar to ambient hexane (Gupta, 2005). Hence, for our application of coal beneficiation, subcritical conditions (e.g., 300 ^{o}C) may provide a conducive solvent atmosphere where various ionic species are effectively solubilized in the fluid and removed.

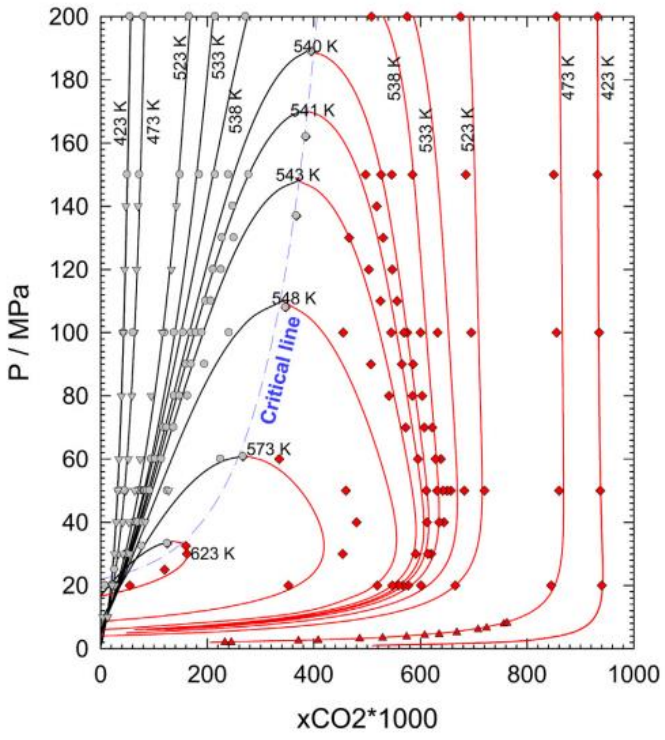

Figure 9: Pressure-mole fraction phase diagram of the CO_2-H_2O system at temperatures of 423 K to 623 K and pressures up to 200 MPa. The isotherms on the left of the critical line stand for the bubble point lines of CO_2 saturated water, and the isotherms on the right of the critical line stand are dew point lines of the H_20 saturated supercritical CO_2. (Zhao et al. 2016).

Chapter 2: Reaction and Phase Equilibria in ScWC Extraction

The proposed extraction utilizes favorable reaction and thermodynamic phase equilibria environment in the supercritical water and carbon dioxide (ScWC). There are three noticeable elements to the ScWC medium: (a) ionization due to reactions among H_2O and CO_2 molecules, (b) reactions with the coal matrix, and (c) phase equilibrium which determines the phase density (i.e., vapor, liquid, supercritical) important for the solublization of the extracted components.

2.1 Ionization Reactions in Supercritical water and carbon dioxide (ScWC)

Self-ionization of water to form H+ and OH- ions and reaction of water with CO_2 leads to the following ionization reactions:

Reference: Conrad, Jacy; Sasidharanpillai, Swaroop; and Tremaine, Peter R. ; Second Dissociation Constant of Carbonic Acid in H2O and D2O from 150 to 325 °C at p = 21 MPa Using Raman Spectroscopy and a Sapphire-Windowed Flow Cell, J. Phys. Chem. B 2020, 124, 2600−2617.

Reaction 1a (ionization of carbonic acid):

$$CO_2(aq) + H_2O \leftrightarrow HCO_3^- + H^+ \qquad K_{1a,H} = (a_{H+}\, a_{HCO3^-})/(a_{CO2}\, a_{H2O})$$

Reaction 2a (dissociation of carbonic acid):

$$HCO_3^- \leftrightarrow CO_3^{2-} + H^+ \qquad K_{2a,H} = (a_{H+}\, a_{CO3^{2-}})/(a_{HCO3^-})$$

Reaction 2b (hydrolysis of carbonate):

$$CO_3^{2-} + H_2O \leftrightarrow HCO_3^- + OH^- \qquad K_{2b,OH} = (a_{HCO3^-}\, a_{OH^-})/(a_{CO3^{2-}}\, a_{H2O})$$

Reaction 3 (ionization of water):

$H_2O \leftrightarrow H^+ + OH^-$ $K_{3,H} = (a_{H+}\ a_{OH^-})/(a_{H2O})$

Equilibrium data for reaction 1a:

The ionization of carbonic acid to produce HCO_3^- and H^+ ions has been reported as:

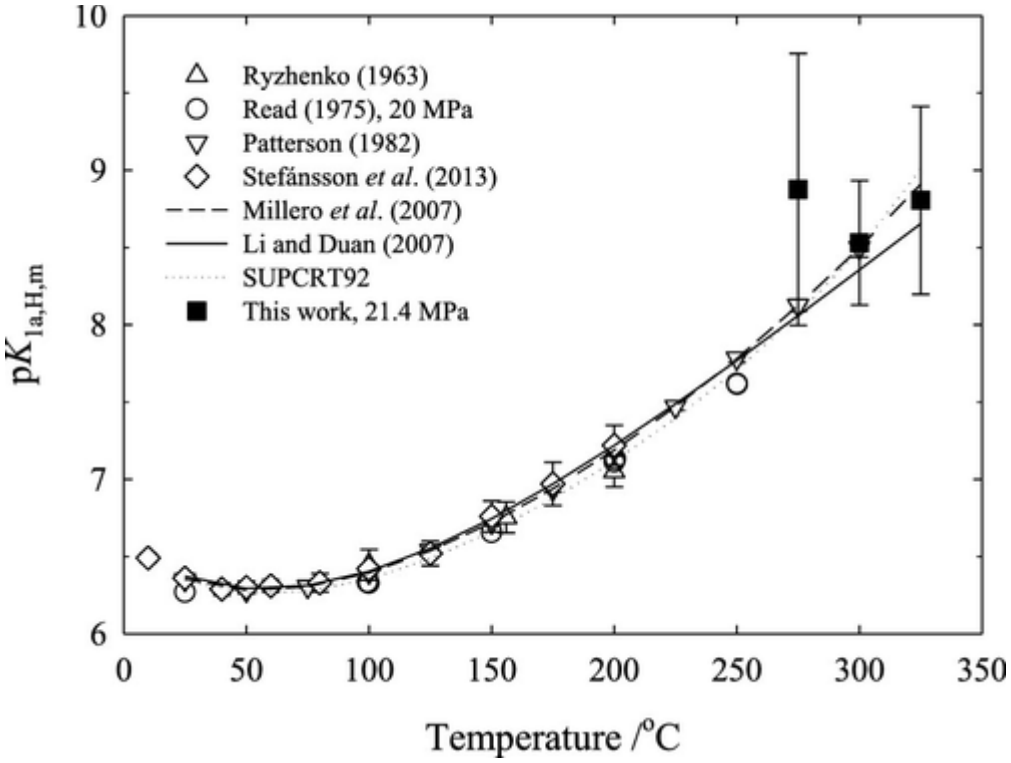

Figure 12. Literature results (24−27,32,33) and the new high-temperature results from this work at 21.4 MPa for the ionization constant of the reaction CO2(aq) + H2O ⇌ HCO3– + H+ plotted against temperature. All studies are at saturation vapor pressure except for where noted in the legend. (Conrad 2020)

T (oC)	**pK1a = -logK1a**
0	6.4
100	6.45
150	6.7
200	7.15

250 7.65

300 8.5

350 9.25

Equilibrium data for reaction 2a:

The dissociation of carbonic acid to produce CO_3^{--} and H^+ ions has been reported as

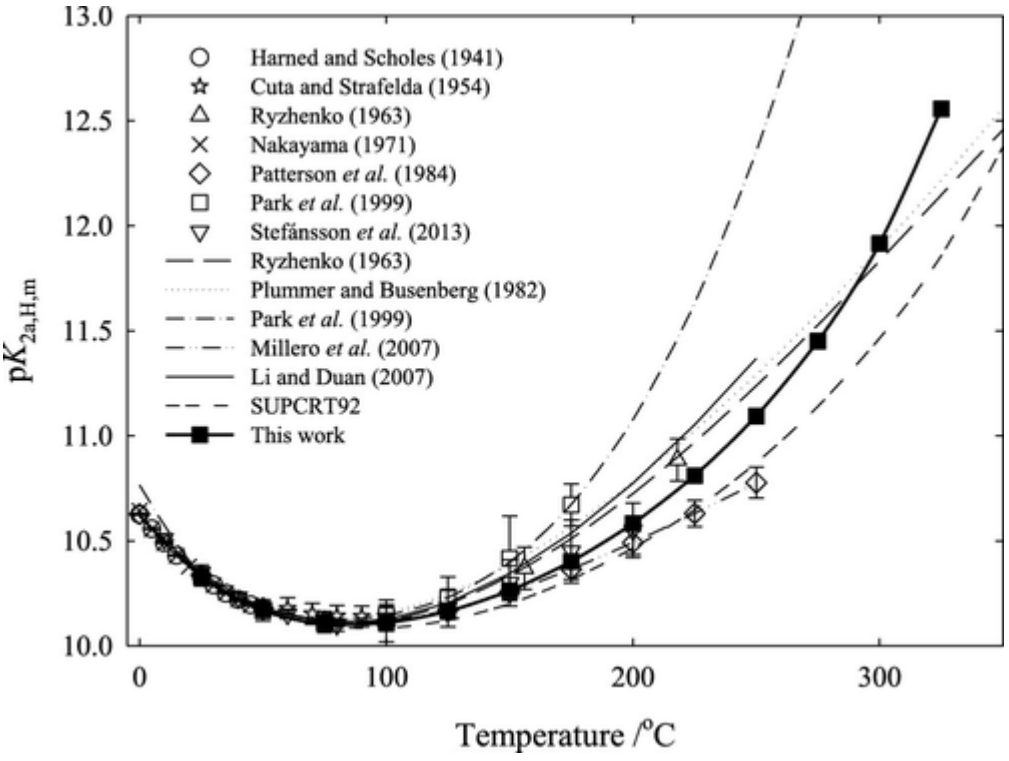

Figure 13. Experimental results(18,19,21−25) and models(33−35) for the second ionization constant of carbonic acid, HCO3– ⇌ CO32– + H+, plotted with the new high-temperature results from this work at saturation vapor pressure on a molality concentration basis (Conrad 2020)

T (oC) pK2a = -logK2a

0 10.65

100 10.15

150 10.45

200 10.75

250 11.35

300 11.9

350 12.55

Equilibrium data for reaction 2b:

The hydrolysis of carbonate to produce HCO3- and OH- is reported as

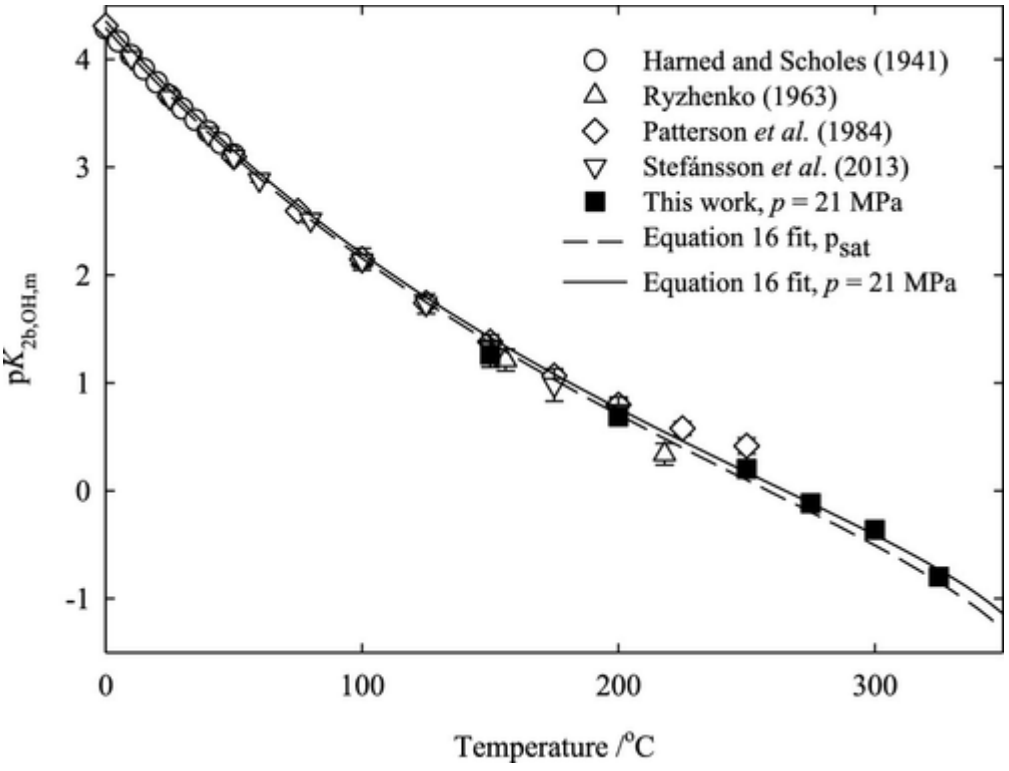

Figure 14. Light water pK2b,OH,m values for CO32– + H2O ⇌ HCO3– + OH– from this work at 21 MPa and from other studies(18,22,24,25) at saturation vapor pressure. The eq 16 fit results are shown at 21 MPa by the solid line and at saturation vapor pressure by the dashed line. (Conrad 2020)

T(oC) pK2b = -logK2b

0 4.28

100	2.15
150	1.37
200	0.705
250	0.098
300	-0.51
350	-0.85

Equilibrium data for reaction 3:

The ionization of water to produce H+ and OH- is reported as:

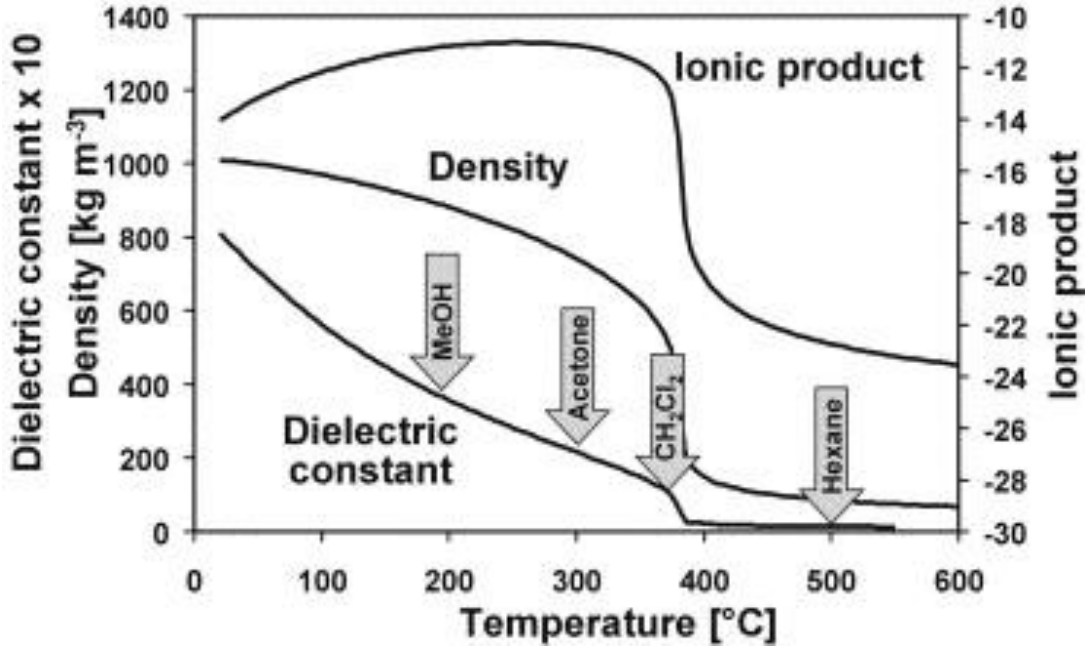

Fig. 15. Physical properties of water at a pressure of 24 MPa versus temperature. Dielectric constants of typical organic solvents at room temperature are indicated. (Kritzer 2001)

T (oC) pK3 = -logK3

0	14.9
100	12.3
150	11.5
200	11.2
250	10.9
300	11.1
350	11.8

2.2 Reactions with the coal components

In the proposed ScWC process, water molecule dissociates to form hydrogen ion and hydroxyl ion that both participate in further extraction reactions. At room temperature, the ions are in small concentration, and the dissociation increased with temperature upto about 300 ^{o}C and then it rapidly drops, as shown in Figure 1 (Kritzer et al. 2001). The concentration of various ions follow a similar path. Coal contains metal elements (i.e., ash content) in addition to carbon and hydrocarbons. Carbonic acid can donate one or two hydrogen atoms in order to dissolve metals into solution or to form carbonate salts. (M = Ca, Mg, etc.)

$$CO_3^{2-}{}_{(aq)} + M^{2+}{}_{(mineral)} \rightarrow MCO_{3\,(s)} \quad (5)$$

$$MCO_{3\,(s)} + H_2CO_{3\,(aq)} \rightleftharpoons M^{2+}{}_{(aq)} + 2HCO_3^{-}{}_{(aq)} \quad (6)$$

$$MCO_{3\,(s)} + \text{heat} \rightarrow MO \quad (7)$$

The CO_2-H_2O mixture is acidic which will help to break down complex mineral structure and provide access to metal ions. Many complex reactions have been hypothesized regarding the

specific forms of sulfur. Although this paper does not attempt to study these reactions, a comprehensive analysis of the reaction network can further help understand the molecular mechanism involved so that a rational design for industrial level extraction plants can be made.

For pyrite, iron and sulfur can react with various forms of hydrogen, carbon, and oxygen ions to ultimately form iron, iron sulfates, iron oxides, and iron salts. Sulfur in pyrite may be converted into sulfate by free oxygen or to hydrogen sulfide by hydrogen ions based off of pyrite breakdown reactions in Steel et al. 2001. Reactive sulfur species COS may also be formed, via a network of reactions as,

$$2FeS_2 + 3H_2CO_{3\,(aq)} \rightarrow 2Fe^{3+} + 3H_2S + S + 3\,CO_3^{2-} \quad 8$$

$$2FeS_2 + 2H_2O + 3CO_2 \rightarrow 2Fe^{3+} + 4SO_4^{2-} + 2H^+ + 3CO \quad 9$$

$$FeS_2 + H_2 \rightarrow FeS + H_2S \quad 10$$

$$FeS + H_2 \rightarrow Fe + H_2S \quad 11$$

$$SO_2 + H_2O \rightleftharpoons H_2SO_3 \quad 12$$

$$SO_2 + H_2O + \tfrac{1}{2}O_2 \rightleftharpoons H_2SO_4 \quad 13$$

$$SO_2 + 2H_2O \rightleftharpoons H_2 + H_2SO_4 \quad 14$$

$$3SO_2 + 2H_2O \rightleftharpoons S + 2H_2SO_4 \quad 15$$

$$4SO_2 + 4H_2O \rightleftharpoons 3H_2SO_4 + H_2S \quad 16$$

$$H_2S + CO \rightarrow COS + H_2 \quad 17$$

$$H_2S + CO_2 \rightarrow COS + H_2O \quad 18$$

$$RSH + H_2O \rightarrow ROH + H_2S \quad (19)$$

$$RSH + CO_2 \rightarrow ROH + COS \quad (20)$$

Organic sulfur is found in coal as mercaptans (RSH), disulfides (RS-S-R'), sulfides (R-S-R'), and thiophenes (heterocyclic). Organic sulfur is thus integrated into the carbon structure and difficult to remove. Oxidative ions convert organic sulfur to sulfates which can be dissolved in water or form sulfur dioxide. Interaction of fluid with the coal may also cause lower organics to liquify or gasify to produce carbon dioxide, hydrogen gas, or methane. More complex studies of the reactions involved can be found in other recent studies (Morimoto et al. 2006; Tian et al. 2016; Zhang et al. 2018).

2.3 Phase Equilibria of CO_2-H_2O mixtures

Carbon dioxide has critical point of 31.1 ^oC and 74 bar which is mild in process conditions, whereas water has high critical point 374 °C and 221 bar which is high in process conditions. A mixture of the two, depending upon the relative composition, the mixture can exit as a single liquid phase, single vapor pressure, two vapor-liquid phases, or a single supercritical phase. Such a variation in the physical behavior gives rise to a degree of choice and control on what is required for a given application. For example, the liquid phase can stabilize the ions hence, ionization is present. On the other hand, vapor phase, in general, cannot stabilize the ions, hence the ionization is suppressed.

To further understand the behavior, we have carried out chemical reaction equilibria and fluid phase equilibria simultaneous calculations using the commercial process simulator Apsen+ and the results for selected CO_2/H_2O ratios and process conditions are shown below. The

calculations show that the ionic content is strong with temperature up to 275℃. At 300℃ and beyond, the fluid becomes a gas and no longer has the density to stabilize ions. This calculation is does not account for supercritical fluid, but does highlight an important phenomenon. If the energy of the supercritical fluid is further increased, the effectiveness of the fluid as an ionic solution will decrease because the density of the fluid will decrease and the fluid will act more closely to a gas. The liquid concentration calculations below may be helpful to groups considering carbon dioxide mixed solvent for new biomass studies.

Aspen+ model selection:

Electrolyte NRTL (Non-Randon Two-Liquid) theory with Redlich-Kong equation of state

Vapor equation of state: ESRK

Liquid activity coefficient: GMENRTL

Liquid molar enthalpy: HLMXELC

Liquid molar volume: VLMXELC with pointing correction

Ionization equilibrium reactions:

$H_2O + CO_2 \leftrightarrow HCO_3^- + H^+$

$\ln(Ka1) = 231.465 - 12092.1/T - 36.7816 \ln(T)$

$HCO_3^- \leftrightarrow CO_3^{--} + H^+$

$\ln(Ka2) = 216.05 - 12431.7/T - 35.4819 \ln(T)$

$H_2O \leftrightarrow OH^- + H^+$

$$\ln(Ka3) = 132.899 - 13445.9/T - 22.4773 \ln(T)$$

where, T is in Kelvin and Ka in mole fraction unit

Process flow diagram for equilibria calculations:

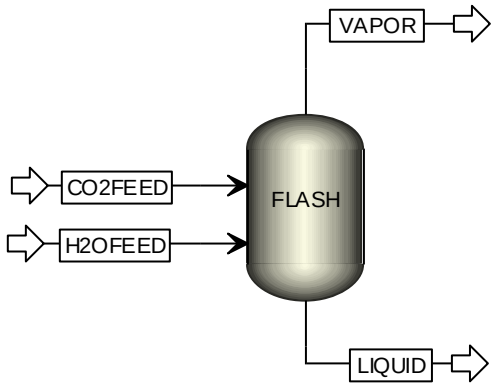

Here the flash unit received the CO_2 and H_2O feed and then they are equilibrated both in terms of chemical ionization and chemical potentials in the fluid phases. Two output, vapor phase and liquid phase, exit the unit. Theses phases are in equilibrium.

Common/fixed process conditions for all calculations:

H_2O rate = 1 kmol/hr

Pressure = 143 bar

Table 2: Aspen Calculations for CO_2/H_20 Mixtures

Calculation 1: CO2 rate = 0.1 kmol/hr and T = 25 ºC

Stream		**CO2 Feed**	**H2O Feed**	**Liquid Outlet**	**Vapor Outlet**

Phase		Liquid Phase	Liquid Phase	Liquid Phase	
Temperature	C	25	25	25	
Pressure	bar	143	143	143	143
Molar Vapor Fraction		0	0	0	
Molar Liquid Fraction		1	1	1	
Molar Solid Fraction		0	0	0	
Mass Vapor Fraction		0	0	0	
Mass Liquid Fraction		1	1	1	
Mass Solid Fraction		0	0	0	
Molar Enthalpy	kcal/mol	-95.5054872	-68.255076	-72.01593382	
Mass Enthalpy	kcal/kg	-2170.09591	-3788.73246	-3533.931495	
Molar Entropy	cal/mol-K	-12.4167858	-38.9889466	-39.95073707	
Mass Entropy	cal/gm-K	-0.28213684	-2.16421541	-1.960443481	
Molar Density	kmol/cum	16.27407303	55.69934794	45.6467383	
Mass Density	kg/cum	716.2186991	1003.439347	930.2083217	
Enthalpy Flow	Gcal/hr	-0.00955055	-0.06825508	-0.079217527	
Average MW		44.0098	18.01527997	20.37841818	
Mole Flows	kmol/hr	0.1	1.000000002	1.1	0
H2O	kmol/hr	0	0.999999998	0.999997034	0
CO2	kmol/hr	0.1	0	0.099997034	0
H+	kmol/hr	0	1.81E-09	2.97E-06	0
OH-	kmol/hr	0	1.81E-09	6.82E-14	0
HCO3-	kmol/hr	0	0	2.97E-06	0
CO3--	kmol/hr	0	0	3.12E-14	0

Calculation 2: CO2 rate = 0.5 kmol/hr and T = 25 ºC

Stream		**CO2 Feed**	**H2O Feed**	**Liquid Outlet**	**Vapor Outlet**
Phase		Liquid Phase	Liquid Phase	Liquid Phase	
Temperature	C	25	25	25	
Pressure	bar	143	143	143	143
Molar Vapor Fraction		0	0	0	
Molar Liquid Fraction		1	1	1	
Molar Solid Fraction		0	0	0	
Mass Vapor Fraction		0	0	0	
Mass Liquid Fraction		1	1	1	
Mass Solid Fraction		0	0	0	

Molar Enthalpy	kcal/mol	-95.5054872	-68.255076	-80.74640572	
Mass Enthalpy	kcal/kg	-2170.09591	-3788.73246	-3026.463364	
Molar Entropy	cal/mol-K	-12.4167858	-38.9889466	-39.43388181	
Mass Entropy	cal/gm-K	-0.28213684	-2.16421541	-1.478024904	
Molar Density	kmol/cum	16.27407303	55.69934794	30.81522531	
Mass Density	kg/cum	716.2186991	1003.439347	822.153909	
Enthalpy Flow	Gcal/hr	-0.04775274	-0.06825508	-0.121119609	
Average MW		44.0098	18.01527997	26.68012	
Mole Flows	kmol/hr	0.5	1.000000002	1.5	0
H2O	kmol/hr	0	0.999999998	0.999999795	0
CO2	kmol/hr	0.5	0	0.499999795	0
H+	kmol/hr	0	1.81E-09	2.05E-07	0
OH-	kmol/hr	0	1.81E-09	6.04E-16	0
HCO3-	kmol/hr	0	0	2.05E-07	0
CO3--	kmol/hr	0	0	2.54E-18	0

Calculation 3: CO2 rate = 1 kmol/hr and T = 25 ºC

Stream		**CO2 Feed**	**H2O Feed**	**Liquid Outlet**	**Vapor Outlet**
Phase		Liquid Phase	Liquid Phase	Liquid Phase	
Temperature	C	25	25	25	
Pressure	bar	143	143	143	143
Molar Vapor Fraction		0	0	0	
Molar Liquid Fraction		1	1	1	
Molar Solid Fraction		0	0	0	
Mass Vapor Fraction		0	0	0	
Mass Liquid Fraction		1	1	1	
Mass Solid Fraction		0	0	0	
Molar Enthalpy	kcal/mol	-95.5054872	-68.255076	-85.70445397	
Mass Enthalpy	kcal/kg	-2170.09591	-3788.73246	-2763.541908	
Molar Entropy	cal/mol-K	-12.4167858	-38.9889466	-36.18194972	
Mass Entropy	cal/gm-K	-0.28213684	-2.16421541	-1.166687724	
Molar Density	kmol/cum	16.27407303	55.69934794	25.18861144	
Mass Density	kg/cum	716.2186991	1003.439347	781.1628198	

Enthalpy Flow	Gcal/hr	-0.09550549	-0.06825508	-0.171408908	
Average MW		44.0098	18.01527997	31.01254	
Mole Flows	kmol/hr	1	1.000000002	2	0
H2O	kmol/hr	0	0.999999998	0.999999981	0
CO2	kmol/hr	1	0	0.999999981	0
H+	kmol/hr	0	1.81E-09	1.89E-08	0
OH-	kmol/hr	0	1.81E-09	2.54E-17	0
HCO3-	kmol/hr	0	0	1.89E-08	0
CO3--	kmol/hr	0	0	9.22E-22	0

Calculation 4: CO2 rate = 0.1 kmol/hr and T = 200 ºC

Stream		**CO2 Feed**	**H2O Feed**	**Liquid Outlet**	**Vapor Outlet**
Phase		Vapor Phase	Liquid Phase	Liquid Phase	Vapor Phase
Temperature	C	200	200	200	200
Pressure	bar	143	143	143	143
Molar Vapor Fraction		1	0	0	1
Molar Liquid Fraction		0	1	1	0
Molar Solid Fraction		0	0	0	0
Mass Vapor Fraction		1	0	0	1
Mass Liquid Fraction		0	1	1	0
Mass Solid Fraction		0	0	0	0
Molar Enthalpy	kcal/mol	-92.9056457	-65.0719877	-65.26549649	-86.25416433
Mass Enthalpy	kcal/kg	-2111.02177	-3612.04436	-3594.059721	-2208.676382
Molar Entropy	cal/mol-K	-5.53172728	-30.6085351	-30.55893818	-7.155084353
Mass Entropy	cal/gm-K	-0.12569308	-1.69903195	-1.682828673	-0.183217424
Molar Density	kmol/cum	4.227639985	48.52558072	47.59499387	4.670235765
Mass Density	kg/cum	186.0575902	874.2018869	864.2902863	182.3840226
Enthalpy Flow	Gcal/hr	-0.00929056	-0.06507199	-0.064166712	-0.010077558
Average MW		44.0098	18.01527924	18.15926878	39.052423
Mole Flows	kmol/hr	0.1	1.000000042	0.983164394	0.116835606
H2O	kmol/hr	0	0.999999958	0.977689431	0.022281548
CO2	kmol/hr	0.1	0	0.005416921	0.094554058
H+	kmol/hr	0	4.22E-08	2.90E-05	0
OH-	kmol/hr	0	4.22E-08	7.39E-11	0
HCO3-	kmol/hr	0	0	2.90E-05	0
CO3--	kmol/hr	0	0	4.36E-13	0

Calculation 5: CO2 rate = 0.5 kmol/hr and T = 200 ºC

Stream		**CO2 Feed**	**H2O Feed**	**Liquid Outlet**	**Vapor Outlet**
Phase		Vapor Phase	Liquid Phase	Liquid Phase	Vapor Phase
Temperature	C	200	200	200	200
Pressure	bar	143	143	143	143
Molar Vapor Fraction		1	0	0	1
Molar Liquid Fraction		0	1	1	0
Molar Solid Fraction		0	0	0	0
Mass Vapor Fraction		1	0	0	1
Mass Liquid Fraction		0	1	1	0
Mass Solid Fraction		0	0	0	0
Molar Enthalpy	kcal/mol	-92.9056457	-65.0719877	-65.26549648	-86.25416434
Mass Enthalpy	kcal/kg	-2111.02177	-3612.04436	-3594.059722	-2208.676382
Molar Entropy	cal/mol-K	-5.53172728	-30.6085351	-30.55893818	-7.155084352
Mass Entropy	cal/gm-K	-0.12569308	-1.69903195	-1.682828673	-0.183217424
Molar Density	kmol/cum	4.227639985	48.52558072	47.59499391	4.670235765
Mass Density	kg/cum	186.0575902	874.2018869	864.2902868	182.3840226
Enthalpy Flow	Gcal/hr	-0.04645282	-0.06507199	-0.057972422	-0.05276553
Average MW		44.0098	18.01527924	18.15926877	39.052423
Mole Flows	kmol/hr	0.5	1.000000042	0.888255278	0.611744723
H2O	kmol/hr	0	0.999999958	0.883308837	0.116664944
CO2	kmol/hr	0.5	0	0.004894002	0.495079779
H+	kmol/hr	0	4.22E-08	2.62E-05	0
OH-	kmol/hr	0	4.22E-08	6.68E-11	0
HCO3-	kmol/hr	0	0	2.62E-05	0
CO3--	kmol/hr	0	0	3.94E-13	0

Calculation 6: CO2 rate = 1 kmol/hr and T = 200 ºC

Stream		**CO2 Feed**	**H2O Feed**	**Liquid Outlet**	**Vapor Outlet**
Phase		Vapor Phase	Liquid Phase	Liquid Phase	Vapor Phase
Temperature	C	200	200	200	200
Pressure	bar	143	143	143	143
Molar Vapor Fraction		1	0	0	1
Molar Liquid Fraction		0	1	1	0

Molar Solid Fraction		0	0	0	0
Mass Vapor Fraction		1	0	0	1
Mass Liquid Fraction		0	1	1	0
Mass Solid Fraction		0	0	0	0
Molar Enthalpy	kcal/mol	-92.9056457	-65.0719877	-65.26549637	-86.25416442
Mass Enthalpy	kcal/kg	-2111.02177	-3612.04436	-3594.059732	-2208.67638
Molar Entropy	cal/mol-K	-5.53172728	-30.6085351	-30.55893821	-7.155084324
Mass Entropy	cal/gm-K	-0.12569308	-1.69903195	-1.682828682	-0.183217423
Molar Density	kmol/cum	4.227639985	48.52558072	47.59499444	4.670235757
Mass Density	kg/cum	186.0575902	874.2018869	864.2902924	182.3840226
Enthalpy Flow	Gcal/hr	-0.09290565	-0.06507199	-0.050229558	-0.106125495
Average MW		44.0098	18.01527924	18.15926869	39.05242307
Mole Flows	kmol/hr	1	1.000000042	0.769618883	1.230381117
H2O	kmol/hr	0	0.999999958	0.765333098	0.234644185
CO2	kmol/hr	1	0	0.004240351	0.995736932
H+	kmol/hr	0	4.22E-08	2.27E-05	0
OH-	kmol/hr	0	4.22E-08	5.78E-11	0
HCO3-	kmol/hr	0	0	2.27E-05	0
CO3--	kmol/hr	0	0	3.41E-13	0

Calculation 7: CO2 rate = 0.1 kmol/hr and T = 250 ºC

Stream		**CO2 Feed**	**H2O Feed**	**Liquid Outlet**	**Vapor Outlet**
Phase		Vapor Phase	Liquid Phase	Liquid Phase	Vapor Phase
Temperature	C	250	250	250	250
Pressure	bar	143	143	143	143
Molar Vapor Fraction		1	0	0	1
Molar Liquid Fraction		0	1	1	0
Molar Solid Fraction		0	0	0	0
Mass Vapor Fraction		1	0	0	1
Mass Liquid Fraction		0	1	1	0
Mass Solid Fraction		0	0	0	0
Molar Enthalpy	kcal/mol	-92.2610889	-64.0899425	-64.11885093	-78.09757876
Mass Enthalpy	kcal/kg	-2096.37601	-3557.5326	-3554.893549	-2333.671234
Molar Entropy	cal/mol-K	-4.23632928	-28.6366067	-28.62681951	-8.34646965
Mass Entropy	cal/gm-K	-0.09625877	-1.58957331	-1.587135367	-0.249404866

Molar Density	kmol/cum	3.620470603	45.00002091	44.88192572	4.281257115
Mass Density	kg/cum	159.3361872	810.6879336	809.5256481	143.2746009
Enthalpy Flow	Gcal/hr	-0.00922611	-0.06408995	-0.059826239	-0.013038214
Average MW		44.0098	18.01527904	18.03678508	33.4655446
Mole Flows	kmol/hr	0.1	1.000000053	0.933052269	0.166947732
H2O	kmol/hr	0	0.999999947	0.932272267	0.067719639
CO2	kmol/hr	0.1	0	0.000763814	0.099228092
H+	kmol/hr	0	5.31E-08	8.09E-06	0
OH-	kmol/hr	0	5.31E-08	3.38E-10	0
HCO3-	kmol/hr	0	0	8.09E-06	0
CO3--	kmol/hr	0	0	1.27E-13	0

Calculation 8: CO2 rate = 0.5 kmol/hr and T = 250 ºC

Stream		**CO2 Feed**	**H2O Feed**	**Liquid Outlet**	**Vapor Outlet**
Phase		Vapor Phase	Liquid Phase	Liquid Phase	Vapor Phase
Temperature	C	250	250	250	250
Pressure	bar	143	143	143	143
Molar Vapor Fraction		1	0	0	1
Molar Liquid Fraction		0	1	1	0
Molar Solid Fraction		0	0	0	0
Mass Vapor Fraction		1	0	0	1
Mass Liquid Fraction		0	1	1	0
Mass Solid Fraction		0	0	0	0
Molar Enthalpy	kcal/mol	-92.2610889	-64.0899425	-64.11885119	-78.09765314
Mass Enthalpy	kcal/kg	-2096.37601	-3557.5326	-3554.893526	-2333.669557
Molar Entropy	cal/mol-K	-4.23632928	-28.6366067	-28.62681943	-8.346441196
Mass Entropy	cal/gm-K	-0.09625877	-1.58957331	-1.587135346	-0.249403599
Molar Density	kmol/cum	3.620470603	45.00002091	44.88192465	4.281251637
Mass Density	kg/cum	159.3361872	810.6879336	809.5256376	143.274657
Enthalpy Flow	Gcal/hr	-0.04613054	-0.06408995	-0.042298505	-0.065626312
Average MW		44.0098	18.01527904	18.03678527	33.46560052
Mole Flows	kmol/hr	0.5	1.000000053	0.65968907	0.84031093
H2O	kmol/hr	0	0.999999947	0.659137587	0.340856691
CO2	kmol/hr	0.5	0	0.000540039	0.499454239
H+	kmol/hr	0	5.31E-08	5.72E-06	0

OH-	kmol/hr	0	5.31E-08	2.39E-10	0
HCO3-	kmol/hr	0	0	5.72E-06	0
CO3--	kmol/hr	0	0	8.99E-14	0

Calculation 9: CO2 rate = 1 kmol/hr and T = 250 °C

Stream		**CO2 Feed**	**H2O Feed**	**Liquid Outlet**	**Vapor Outlet**
Phase		Vapor Phase	Liquid Phase	Liquid Phase	Vapor Phase
Temperature	C	250	250	250	250
Pressure	bar	143	143	143	143
Molar Vapor Fraction		1	0	0	1
Molar Liquid Fraction		0	1	1	0
Molar Solid Fraction		0	0	0	0
Mass Vapor Fraction		1	0	0	1
Mass Liquid Fraction		0	1	1	0
Mass Solid Fraction		0	0	0	0
Molar Enthalpy	kcal/mol	-92.2610889	-64.0899425	-64.1188512	-78.09765927
Mass Enthalpy	kcal/kg	-2096.37601	-3557.5326	-3554.893525	-2333.669419
Molar Entropy	cal/mol-K	-4.23632928	-28.6366067	-28.62681943	-8.346438852
Mass Entropy	cal/gm-K	-0.09625877	-1.58957331	-1.587135346	-0.249403494
Molar Density	kmol/cum	3.620470603	45.00002091	44.88192464	4.281251186
Mass Density	kg/cum	159.3361872	810.6879336	809.5256375	143.2746616
Enthalpy Flow	Gcal/hr	-0.09226109	-0.06408995	-0.02038882	-0.13136145
Average MW		44.0098	18.01527904	18.03678528	33.46560513
Mole Flows	kmol/hr	1	1.000000053	0.317984804	1.682015196
H2O	kmol/hr	0	0.999999947	0.317718977	0.682278265
CO2	kmol/hr	1	0	0.000260311	0.999736931
H+	kmol/hr	0	5.31E-08	2.76E-06	0
OH-	kmol/hr	0	5.31E-08	1.15E-10	0
HCO3-	kmol/hr	0	0	2.76E-06	0
CO3--	kmol/hr	0	0	4.33E-14	0

Calculation 10: CO2 rate = 0.1 kmol/hr and T = 300 °C

Stream		**CO2 Feed**	**H2O Feed**	**Liquid Outlet**	**Vapor Outlet**
Phase		Vapor Phase	Liquid Phase	Liquid Phase	Vapor Phase
Temperature	C	300	300	300	300
Pressure	bar	143	143	143	143

Molar Vapor Fraction		1	0	0	1
Molar Liquid Fraction		0	1	1	0
Molar Solid Fraction		0	0	0	0
Mass Vapor Fraction		1	0	0	1
Mass Liquid Fraction		0	1	1	0
Mass Solid Fraction		0	0	0	0
Molar Enthalpy	kcal/mol	-91.6316542	-63.002392	-63.00608826	-66.4379559
Mass Enthalpy	kcal/kg	-2082.07386	-3497.16439	-3496.839882	-2636.386095
Molar Entropy	cal/mol-K	-3.08713274	-26.6534131	-26.65185879	-11.71387212
Mass Entropy	cal/gm-K	-0.07014648	-1.47948934	-1.479179002	-0.464829015
Molar Density	kmol/cum	3.194071925	40.20843819	40.19703022	4.208137672
Mass Density	kg/cum	140.5704666	724.36623	724.2704039	106.0467075
Enthalpy Flow	Gcal/hr	-0.00916317	-0.0630024	-0.046529817	-0.024017511
Average MW		44.0098	18.01527895	18.0180078	25.20038929
Mole Flows	kmol/hr	0.1	1.000000059	0.738497148	0.361502853
H2O	kmol/hr	0	0.999999941	0.73841812	0.26158035
CO_2	kmol/hr	0.1	0	7.60E-05	0.099922503
H+	kmol/hr	0	5.85E-08	1.53E-06	0
OH-	kmol/hr	0	5.85E-08	1.29E-09	0
HCO3-	kmol/hr	0	0	1.53E-06	0
CO3--	kmol/hr	0	0	2.89E-14	0

Calculation 11: CO2 rate = 0.5 kmol/hr and T = 300 ºC

Stream		**CO2 Feed**	**H2O Feed**	**Liquid Outlet**	**Vapor Outlet**
Phase		Vapor Phase	Liquid Phase		Vapor Phase
Temperature	C	300	300		300
Pressure	bar	143	143	143	143
Molar Vapor Fraction		1	0		1
Molar Liquid Fraction		0	1		0
Molar Solid Fraction		0	0		0
Mass Vapor Fraction		1	0		1
Mass Liquid Fraction		0	1		0
Mass Solid Fraction		0	0		0
Molar Enthalpy	kcal/mol	-91.6316542	-63.002392		-68.38779495
Mass Enthalpy	kcal/kg	-2082.07386	-3497.16439		-2563.249151

Molar Entropy	cal/mol-K	-3.08713274	-26.6534131		-10.80221787
Mass Entropy	cal/gm-K	-0.07014648	-1.47948934		-0.404878909
Molar Density	kmol/cum	3.194071925	40.20843819		4.051406324
Mass Density	kg/cum	140.5704666	724.36623		108.0920069
Enthalpy Flow	Gcal/hr	-0.04581583	-0.0630024		-0.102581692
Average MW		44.0098	18.01527895		26.68012
Mole Flows	kmol/hr	0.5	1.000000059	0	1.5
H2O	kmol/hr	0	0.999999941	0	1
CO2	kmol/hr	0.5	0	0.00E+00	0.5
H+	kmol/hr	0	5.85E-08	0.00E+00	0
OH-	kmol/hr	0	5.85E-08	0.00E+00	0
HCO3-	kmol/hr	0	0	0.00E+00	0
CO3--	kmol/hr	0	0	0.00E+00	0

Calculation 12: CO2 rate = 1 kmol/hr and T = 300 ºC

Stream		**CO2 Feed**	**H2O Feed**	**Liquid Outlet**	**Vapor Outlet**
Phase		Vapor Phase	Liquid Phase		Vapor Phase
Temperature	C	300	300		300
Pressure	bar	143	143	143	143
Molar Vapor Fraction		1	0		1
Molar Liquid Fraction		0	1		0
Molar Solid Fraction		0	0		0
Mass Vapor Fraction		1	0		1
Mass Liquid Fraction		0	1		0
Mass Solid Fraction		0	0		0
Molar Enthalpy	kcal/mol	-91.6316542	-63.002392		-74.14572671
Mass Enthalpy	kcal/kg	-2082.07386	-3497.16439		-2390.830506
Molar Entropy	cal/mol-K	-3.08713274	-26.6534131		-8.368747571
Mass Entropy	cal/gm-K	-0.07014648	-1.47948934		-0.26985044
Molar Density	kmol/cum	3.194071925	40.20843819		3.719525494
Mass Density	kg/cum	140.5704666	724.36623		115.3519332
Enthalpy Flow	Gcal/hr	-0.09163165	-0.0630024		-0.148291453
Average MW		44.0098	18.01527895		31.01254
Mole Flows	kmol/hr	1	1.000000059	0	2
H2O	kmol/hr	0	0.999999941	0	1

CO2	kmol/hr	1	0	0.00E+00	1
H+	kmol/hr	0	5.85E-08	0.00E+00	0
OH-	kmol/hr	0	5.85E-08	0.00E+00	0
HCO3-	kmol/hr	0	0	0.00E+00	0
CO3--	kmol/hr	0	0	0.00E+00	0

The above calculations provide a map of the ionic conditions fluid densities observed as a function of CO_2/H_2O ratio and temperature. For simplicity, we have kept the pressure for calculation as 143 bar. Also, the liquid phase properties are not too impacted by the pressure. It is also noted that high fluid density is needed to stabilize the ions. In the proposed ScWC process, it is expected that both ionic and non-ionic extractions will play a prominent role.

Chapter 3. Experimental Work

For the experimental work to test out the proposed extraction process, a new apparatus was constructed. Design of the apparatus and it development over time is described below. The concept was tested on a commercial coal obtained from mine in Pennsylvania.

3.1 Materials

Supercritical fluid grade CO_2 and deionized water and their mixtures were used as extraction fluids. The pulverized bituminous coal with particle size 250-1250 micron was obtained from Rosebud Mining Company (Kittanning, PA) identified as Clymer Blend CPA#101315. Nanopure filtered water was used for all testing. High purity SFE grade CO_2 tank with dip tube was provided by Airgas. Coal standard 2683c was acquired from NIST. For analytical work, 70% environmental grade nitric acid from GFS Chemicals was used for ICP-OES. Boric acid was purchased from the American Borate Company, and pure sodium sulfate and sodium hydroxide were purchased from Sigma Aldrich.

3.2 Coal Extraction Apparatus

A semi-continuous coal extractor was designed and built as shown in Figure 3, in which coal powder is packed in the extraction vessel and the extraction fluid is pumped continuously.

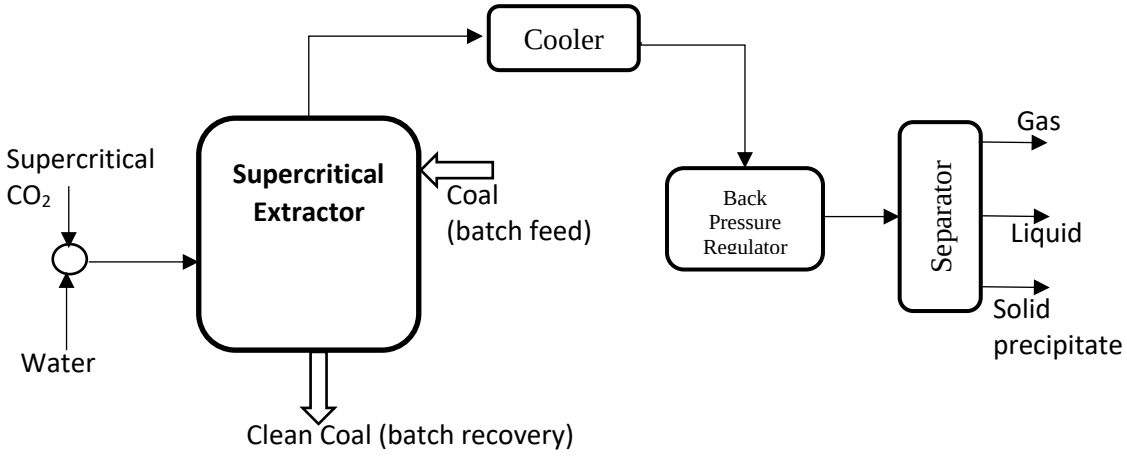

Figure 16. Schematic of the semi-continuous supercritical H_2O-CO_2 (ScWC) extraction of coal

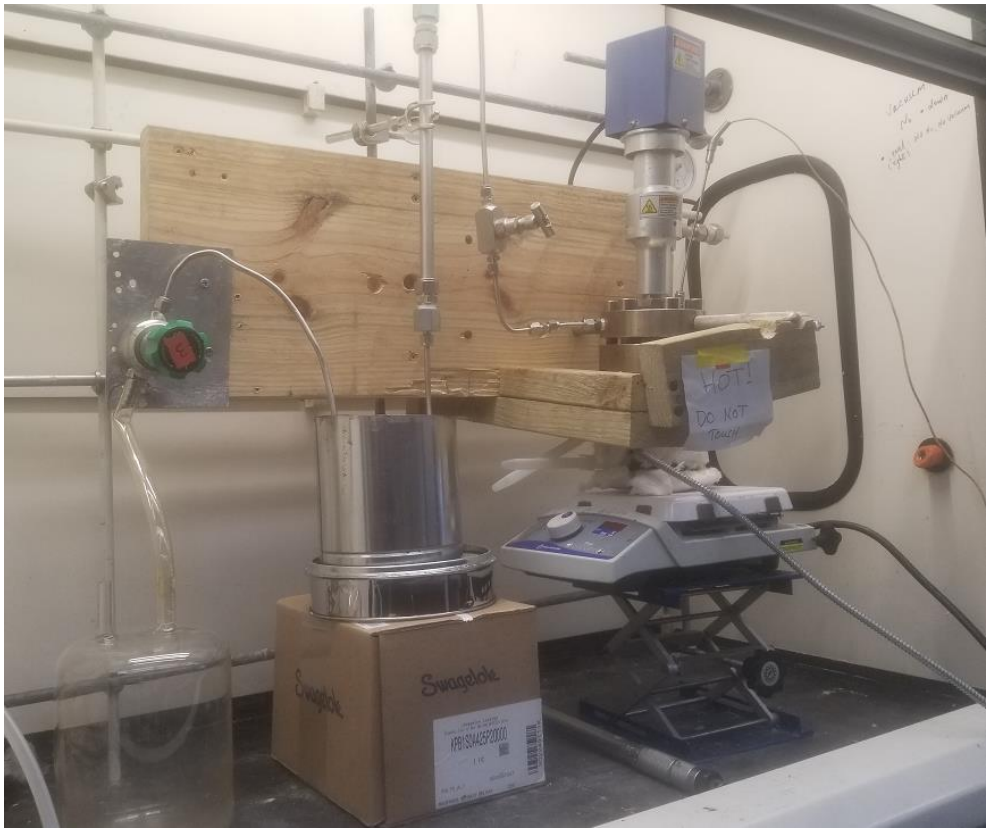

Figure 17. Photograph of the apparatus

Figure 18. Photographs of the CO2 and H2O pumps

A high-pressure hydrothermal reactor (model XHTC400 USP-1200) from Columbia International was used as a flow vessel to extract coal solids. The vessel volume is 250 mL and material of construction is S316 stainless steel. The vessel itself is rated to a maximum continuous working temperature of 400 ℃, maximum temperature of 450 ℃, and a maximum working pressure of 200 bar. A Supercritical 24 constant flow/constant pressure dual-piston pump was used to pressurize the vessel with CO_2. An Eldex 1SMP pump (0-5 mL/min, <200 bar) was used to pump water. The two streams meet at a tee joint that immediately feeds to a check valve at the vessel inlet. The vessel was heated with a Rama 1000W heating band controlled by a temperature controller. A Swagelok KPB1P0A422P20000 backpressure regulator was used to control the

pressure of the outlet. Gas exiting from the regulator was fed to room temperature separator to allow aqueous suspension leachate to separate from gaseous CO_2.

3.3 Typical Experimental Procedure

In a typical extraction, the cooling/chilling unit on the Supercritical 24 pump were turned on and allowed to cool for 20 minutes. The vessel was loaded with about 10-50 grams of pulverized coal and covered with porous glass wool to suppress carryover of the coal particles by the extraction fluid. The vessel was tightened and the backpressure regulator left slightly open. If the extraction called for water, the Eldex pump would be then be primed, turned off, and connected to the vessel inlet. The CO_2 tank was then opened and the pump turned on. The regulator was then closed all the way and checked for zero outlet flow. The vessel was allowed to fully pressurize to 153 bar with only CO_2 over the course of about 25 minutes at which point the backpressure regulator was opened and a steady flow established. The temperature controller was then turned on and set to 75º C. If the extraction called for water, the Eldex pump would also be turned on. Once the vessel reached about 50º C, the setpoint was increased to 175º C and then again to desired set point. Heating to desired set temperature would take about 25 minutes. Extraction time is then considered to be time zero once the vessel has reached the desired temperature. Upon completion of an extraction, both pumps and the heating would be turned off and the CO_2 tank closed. The regulator was loosened to completely depressurize the vessel and then closed to allow the evacuated vessel to cool overnight. Usually, the vessel temperature would increase past reaction temperature at the beginning of cooling as incoming fluid was shut off and no longer provided a heat duty. Coal solids were weighed before and after extraction. Other than solids embedded in

the glass wool used a filter, total coal mass did not seem to change during extraction. Liquid and solid samples would be collected the next day and stored for analysis.

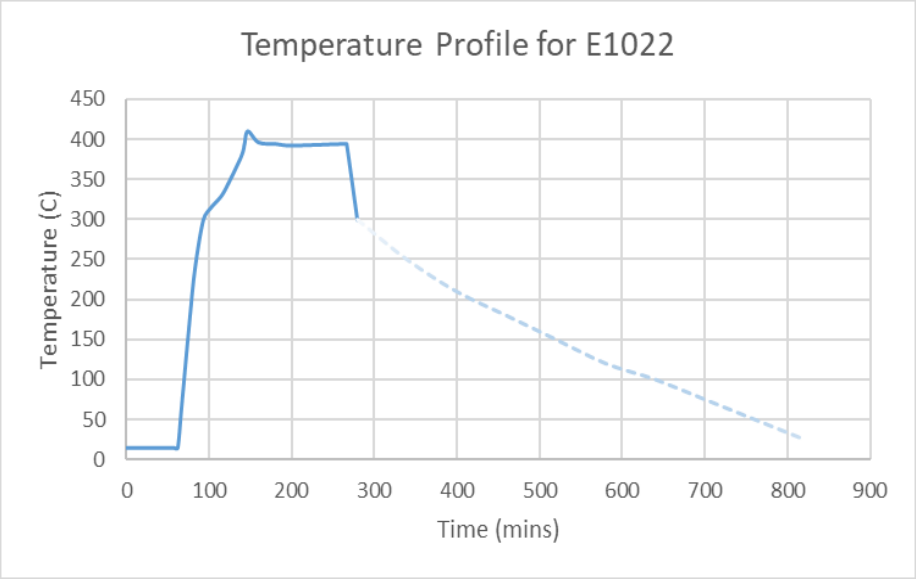

Figure 19: Temperature profile for a typical experiment. Data for experiment E102219 for which the extraction is considered to start at 143 minute timescale. At the end of the experiment forced cooling is achieved with low pressure carbon dioxide flow before ambient cooling.

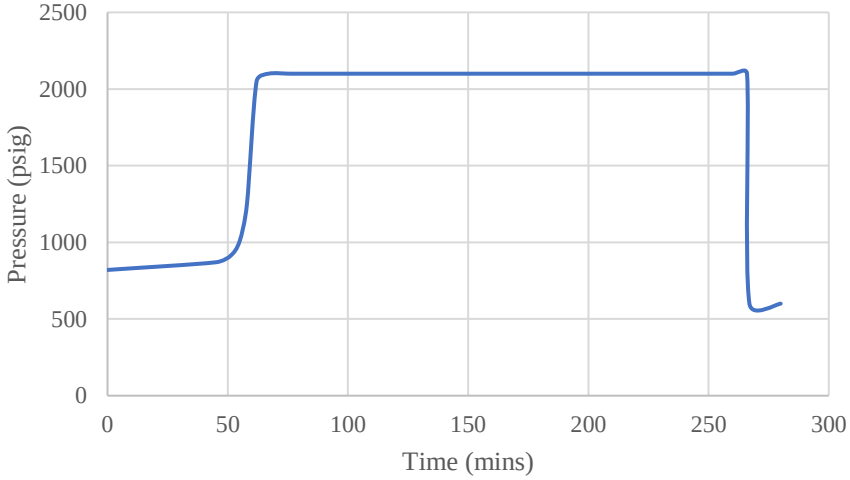

Figure 10: Typical pressure profile. Pressure wavering about 100 psi during the experiment was considered stable.

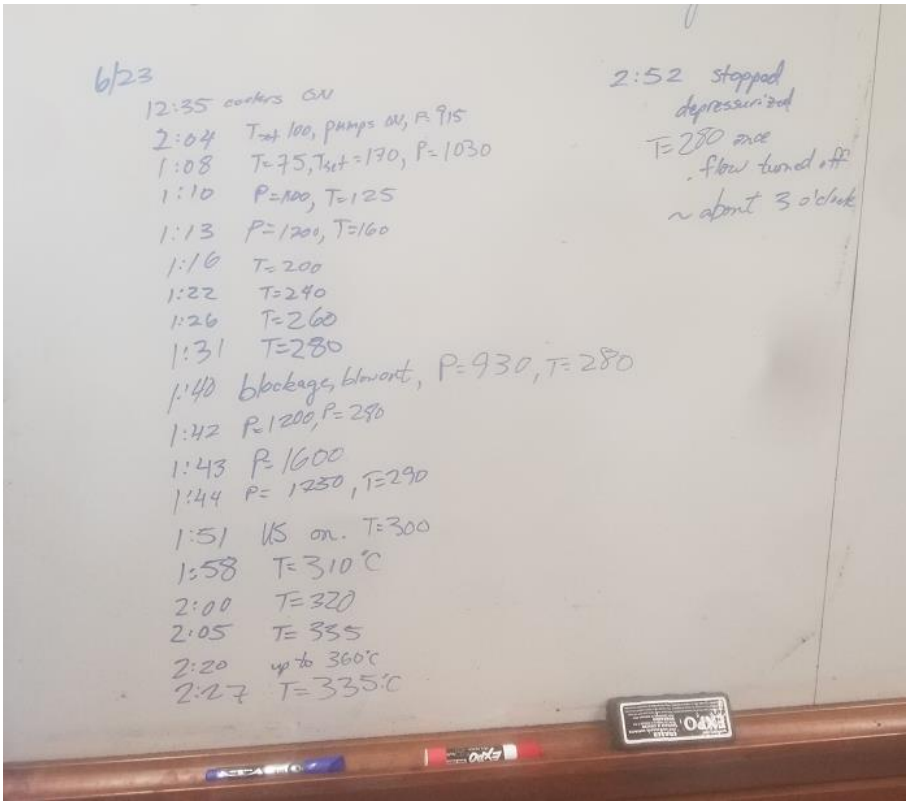

Figure 21 Typical extraction run notes in the laboratory.

3.4 Reactor Development and Troubleshooting

The Columbia vessel and the carbon dioxide pump were left in the lab from a previous student who had used the reactor in a batch setup with a valve at the inlet to the reactor that could be closed when the vessel had been charged with fluid. In order to build a flow type reactor, the pressure gauge and the rupture disc were consolidated to one of the three openings to the vessel. New fittings were used to update the other two openings into inlet and outlet flows. A back-pressure regulator was installed on the outlet to maintain pressure in the vessel. The first struggle with developing the system was actually purchasing incorrectly a front pressure regulator as opposed to back pressure. The backpressure regulator maintains the pressure behind the regulator whereas the font pressure regulator maintains pressure downstream of the regulator. Different

suppliers may specify one but not the other, which lead to ordering a so-called regulator, which was actually a front pressure regulator.

With the correct regulator, the pump was experimented with to become familiar with the vessel pressurizing. It took a couple of months to realize that the pump was not working correctly and needed to be serviced. Without understanding how the pressure should respond to good flow of carbon dioxide, the system would be allowed to pressurize to the liquid carbon dioxide level but the pressure would not build beyond. The pump was sent to the manufacturer for servicing. Servicing the pump involves removing the hood, disconnecting the Peltier element on the front that acts to cool the pump heads, removing the pump casing and check valves, and washing the valves and heads. Very small buildups of contaminant would cause the pump to stop working as the pump heads were only several millimeters diameter. Upon getting the pump back from the manufacturer, the pump worked for a couple weeks and then seemed to be stalled again. In speaking with the service technician, it was discovered that they had reinstalled old seals after cleaning the internal surfaces. The pump manual recommends replacing seals whenever servicing the pump. The manufacturer offered to service the pump again free of charge, but instead the pump has been serviced in house since. Servicing the pump mainly involves thoroughly cleaning the inlet and outlet check valves and replacing seals. It was also decided that the vessel should have a check valve at the inlet to ensure that no solids or fluid from the reactor could back contaminate the pump.

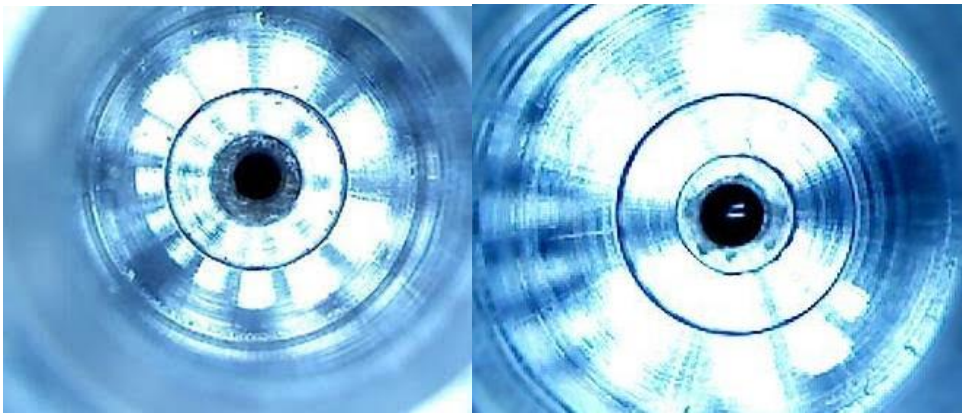

Figure 22: Left: Pinhole for the check valve that has been gunked. Right: Cleaned

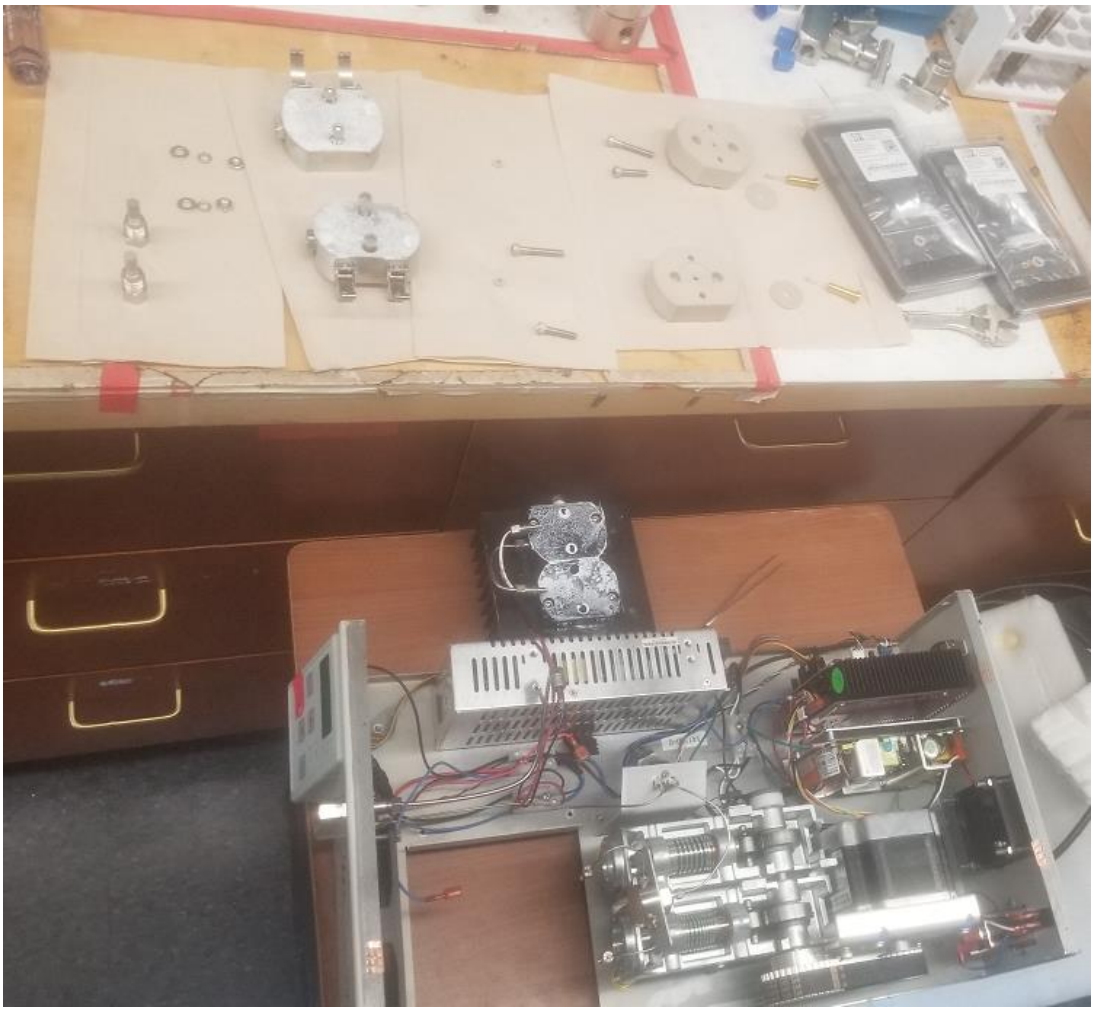

Figure 23. Photograph of the CO_2 pump seals, parts, and internal drive mechanism.

In order to ensure that the carbon dioxide is liquid for pumping, the inlet carbon dioxide to the pump is cooled. Without cooling, the fluid will cavitate and phase shift in the pump instead of being pushed through the check valves. The pump contains an electric cooling Peltier device, but we thought that more cooling may be necessary. A ThermoScientific ACCEL 500 was purchased that could cool refrigerant down to -40 ℃. A large loop was made with the ½" ID plastic tubing for the cooling unit and filled with ethylene glycol. The steel line from the carbon dioxide tank to the pump was then fed into the plastic tubing. Finally, this was the last adjustment necessary to produce good pumping of carbon dioxide.

Figure 24. Photograph of the cooling heat exchanger to liquefy CO2.

In terms of trouble pumping carbon dioxide, we also found that the grade of carbon dioxide tank may be important. At the beginning of the setup, we used a low grade of carbon dioxide and had trouble in concert with a pump that I did not realize was not working. The tank was labeled as

having a dip tube, but that did not seem to be the case. At the same time that the pump came back from servicing, we got a new carbon dioxide tank that was high purity supercritical fluid grade that was specifically manufactured for us with a dip tube. The dip tube ensures that fluid coming from the tank is liquid from the bottom of the tank, and not vapor from the top of the tank. With the newly cleaned and working pump, we did not return to lower grades of carbon dioxide though we probably could have. Experiments have consumed 5 large tanks in the past two years.

With pressurizing understood, we moved to heating the vessel. A new heating jacket was purchased toward the beginning of experiments and has been used with a temperature controller. The setpoint on the controller needed to be increased in stages. The controller would often fail to recognize enough change in temperature and stop itself for 'loop break.' For this reason, it was important to insulate the vessel well. A large sheet of glass wool was purchased for high temperature insulation that is also used as filter inside the vessel. Adding temperature in stages, we found that at 300 ℃ the regulator would stop working correctly because the fluid had reached temperature at the backpressure regulator that would melt the Teflon seal inside. Thus, a cooling coil made from steel tubing was added between the vessel and the regulator that could sit in water. Within three turns of coil, the steel goes from reactor temperature to something I can rest my finger on by evaporating water in the bath.

Figure 2511 Burned out regulator seals from the back pressure regulator

Containment of solids has been the other main experimental challenge. The vessel has a glass containment piece to pack coal into, but the temperature probe and sonicating horn fit down into the glass so forming a good seal is tricky. The best way to contain solids in the vessel was to pack two or three layers of glass wool overtop the coal and try to fit the glass wool snuggly around the horn and thermocouple. Often the vessel would still leak some solids, especially if carbon dioxide pressure decreased sharply and caused fluid to rush to the outlet. For this reason, an inline filter was necessary and installed before the regulator. The filter would need to be disassembled and cleaned with each experiment, and regulators were disassembled and cleaned about once every month or if they became clogged which would prevent the regulator from operating properly. If the regulator became clogged during an experiment, the regulator could be completely closed, and then reopened. Sometimes this would crush the solid enough to get to through, but sometimes the system would build pressure and not be able to get through the regulator even when the regulator was opened. This led to a lot of large depressurizations and scrapped experiments.

Because the vessel in designed for synthesis not extraction, the flow of the fluid does not directly impinge on the solids. Although the flow is pressurized, much of the fluid may escape the vessel without having interacted with the solids as the inlet and outlet to the vessel are both connected to the headspace above the solids packed and filter capped glass container. So, in order to get a better understanding of the actual mass of solvent to mass of coal needed, we installed a wide section of tubing at the outlet of the vessel. Now, coal can be packed into the wide tubing instead of the vessel and the fluid will flow directly through the coal. The tubing is outfitted with stainless steel filters at the bottom of the tube. The tubing can also be packed with glass wool to act as a large filter. Having steel filters ordered and fitted to the wide tubing should alleviate trouble with leaking solids into the fluid stream.

Figure 26. Photograph showing thermos-well containing thermocouple.

Figure 27. Photograph of glass containment vessel stuck to the vessel

Figure 28. Photograph of the broken glass containment vessel.

Figure 29. Photograph of a cleaned coal that has fused due to high temperature.

Figure 30. Outlet aqueous stream containing extracted material.

Figure 31. Photograph of settled extracted material in the outlet water.

Chapter 4. Analysis

Coal was analyzed using the instruments available in chemical engineering, chemistry and nano-characterization center at VCU. For the test that could not be run at VCU, we have gotten commercial testing done from Standard Laboratories, Inc. (South Charleston, WV) which specializes in coal analysis. ASTM methods of standard analysis are listed for coal and followed where applicable.

Moisture Content

Moisture content could be measured by weighing one gram of coal and drying in an oven. Typically, coal would be dried overnight in our vacuum oven at 80℃ and -100 psig. The coal would then be weighed after drying, and the difference attributed to moisture present in the coal assuming complete drying.

Elemental (Ultimate) Analysis

Ultimate analysis is the list by mass of the individual elements in coal. Ultimate analysis is usually obtained by using an elemental analyzer, which pyrolyzes 0.5 – 1.0 mg of substance and then sends vapor through FTIR analysis. With well calibrated spectra and very accurate flow controls, the typical elemental analyzer is able to give carbon, hydrogen, and nitrogen percentages. Some instruments are also able to give sulfur percentages. The balance then can be assumed to be oxygen or oxides. Dr. Bukavekas has a CHN elemental analyzer in the Biology Department, and Old Dominion had a CHNS elemental analyzer.

Heating Value

Heating value of the coal can be experimentally calculated with a bomb calorimeter. Lacking one at VCU, a calculation using the percentages from an ultimate analysis can be used.

Ash Content

Light and heavy metals present in the coal will be left after combustion. To calculate ash percentage, procedure calls for one gram of coal to be loaded into a furnace with flow of air and heated to 750 ℃ for 4 hours, or until no further change in mass. After the carbon, nitrogen, and hydrogen burn off, the remaining solids can be weighed and used to calculate the ash percentage in the coal.

Sulfur Forms

Sulfur can be in the form of pyrite, organic, or sulfate. Total sulfur is found using elemental analysis (ultimate analysis) using pyrolysis and FTIR of vapors. Pyrite and sulfate are found using wet chemistry methods. ASTM methods for pyrite and sulfate quantification are rudimentary and can be influenced by coal structure and the presence of a wide array of interfering elements in coal ash. Standard Laboratories updated methods for pyrite and sulfate quantification were helpful for obtaining data that would have been hard for us to reproduce well. The organic sulfur, containing the most diverse set of bonds, is then calculated as the difference between the total sulfur and the pyrite and sulfate portions.

Chlorine

Commercially analyzed using an ASTM standard and wet chemistry methods.

Mercury

Commercially analyzed using an ASTM standard and wet chemistry methods. ICP-MS also can be used for mercury counts.

Thermogravimetric Analysis

TGA was used to understand the strength of the coal bonds with respect to temperature. In a nitrogen atmosphere, a coal sample of about 3 mg would be slowly heated to 800℃. Typically, the coal will lose mass in three phases. First, moisture vaporizes around 300. In the second phase, volatile sulfur content will decompose, and then finally the volatile carbon portion will evaporate. Thus, the shape of the figures and the final mass remaining are useful tools for analyzing coal.

ICP-OES

Agilent ICP-OES in the Chemisty Instrumentation Lab used to analyze the content of aqueous leachates. A calibration curve was created for sulfur using known dissolved amounts of sodium sulfate in 2% nitric acid. Although this method was used to confirm that sulfur existed in the aqueous leachate, we did not pursue closing vigorous testing of leachates because a significant portion of sulfur may be extracted as gas, but also, a significant portion of the sulfur in the aqueous leachate may evaporate or form salts before the ability to analyze.

Raman Shift

Raman was used to understand changes to the carbon structure that may have been caused by extraction. Also, because the coal contains a wide variety of elements, the influence of

the sample's fluorescence is a weak indicator of ash extraction. Spectra for raw coal had higher counts and more angled baseline than extracted coal due to higher fluorescence of ash metals. For carbon, two characteristic carbon peaks appear at 1350 and 1600 cm^{-1}. With baseline subtracted, the peak heights and ratios are the same between extracted and raw coals. A slight broadening of the peak at 1350 cm^{-1} is noticeable with two shoulder peaks becoming more prominent.

XRD

A PANalytic XRD in VCU's Nano Characterization Center was used to understand the crystallinity of carbon in coal samples before and after extraction. XRD is also helpful for determining the presence of certain minerals, though they did not interest us.

BET

BET was used to determine if the surface area of the coals were greatly affected by extraction. Although raw coal could not be analyzed because of the volatile sulfur portion, the extracted coals could be properly offgassed and analyzed.

ICP-MS

ICP-MS was the most widely used method for us to quantitively analyze our coal in house. This technique allowed us to look directly at the coal mass before and after extraction instead of measuring resultant gas, liquid, and precipitated solids. Carbon, sulfur, and almost all ash metals could be assayed using ICP-MS. Mercury could be analyzed, but not chlorine. Coal

would be dried, pressed into a pellet with boric acid as filler, and then ablated using a laser. Abalated mass would then be swept into a spectrometer and counted.

Approximately 32 mg of dried coal and 593 mg boric acid would be weighed, mixed, and ground together with a high-energy ball mill for 60 seconds with three small balls and three large balls. Then, the mixture would be taken the Chemistry and pressed using a Carver press and an 11 mm die. 3 tons of applied force for 2 minutes was used to fashion pellets.

A 1550W laser (8 J/cm^2) would be focused on the pellet and used to ablate and ionize the pellet surface at low pressure in the presence of plasma gas. Ions are swept by nebulizer gas into the spectroscopy unit and produce counts for each element. A laser spot size of 75 microns was used to ablate 5 mm of pellet to 7.0 mm depth while rastering at 75 micron/s. Line length could be adjusted to obtain an appropriate number of counts to build calibration curves. The experimental error in the sulfur analysis is expected to be 5%.

Pellets were fashioned with various amounts of a NIST coal standard (sulfur, 2 wt.%) in order to create calibration curves with good linearity. From these, we could calculate the total mass of sulfur in a given sample from the sulfur counts. We found that isotopes sulfur 33 and sulfur 34 were both useful, but that sulfur 34 would have an order of magnitude more counts. Although most samples had similar counts for carbon, samples that had been hydrothermally carbonized showed lower carbon counts. For these samples(15-E062519 and 23-E102219), the carbon was more resistant to ablation, and the sulfur values were calculated with respect to the amount of carbon that was actually ablated.

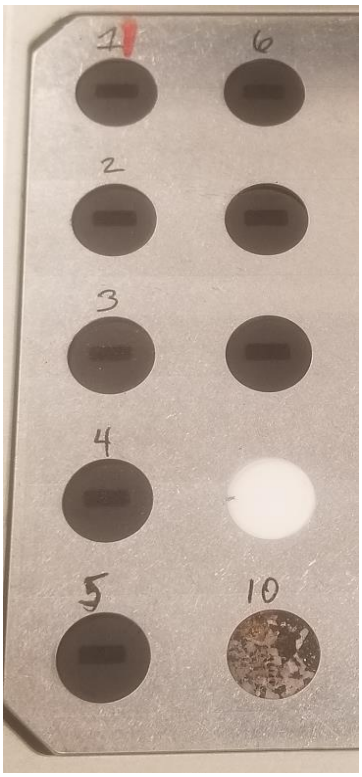

Figure 32. Photograph showing coal pellet that have gone through laser ablation test.

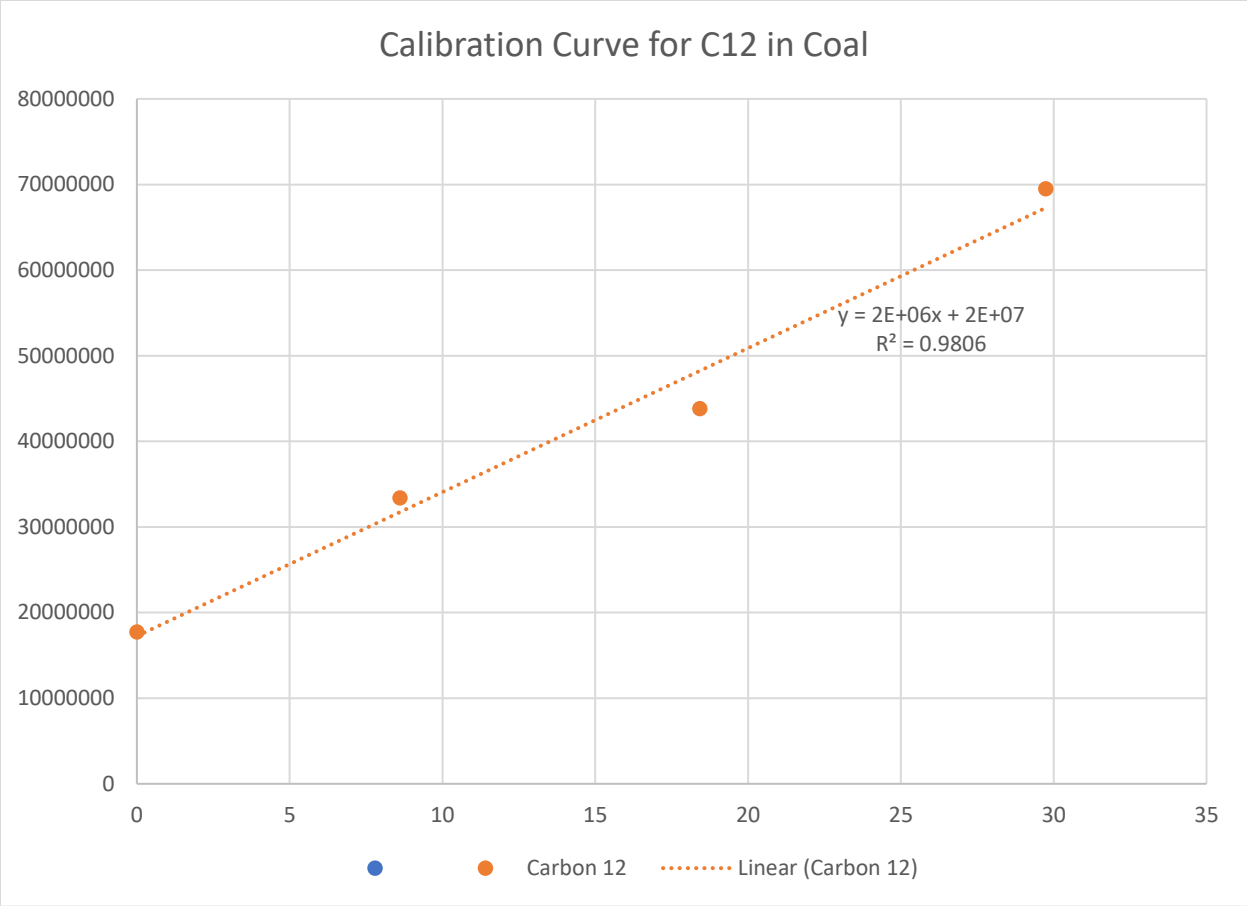

Figure 33. Carbon Calibration Curve

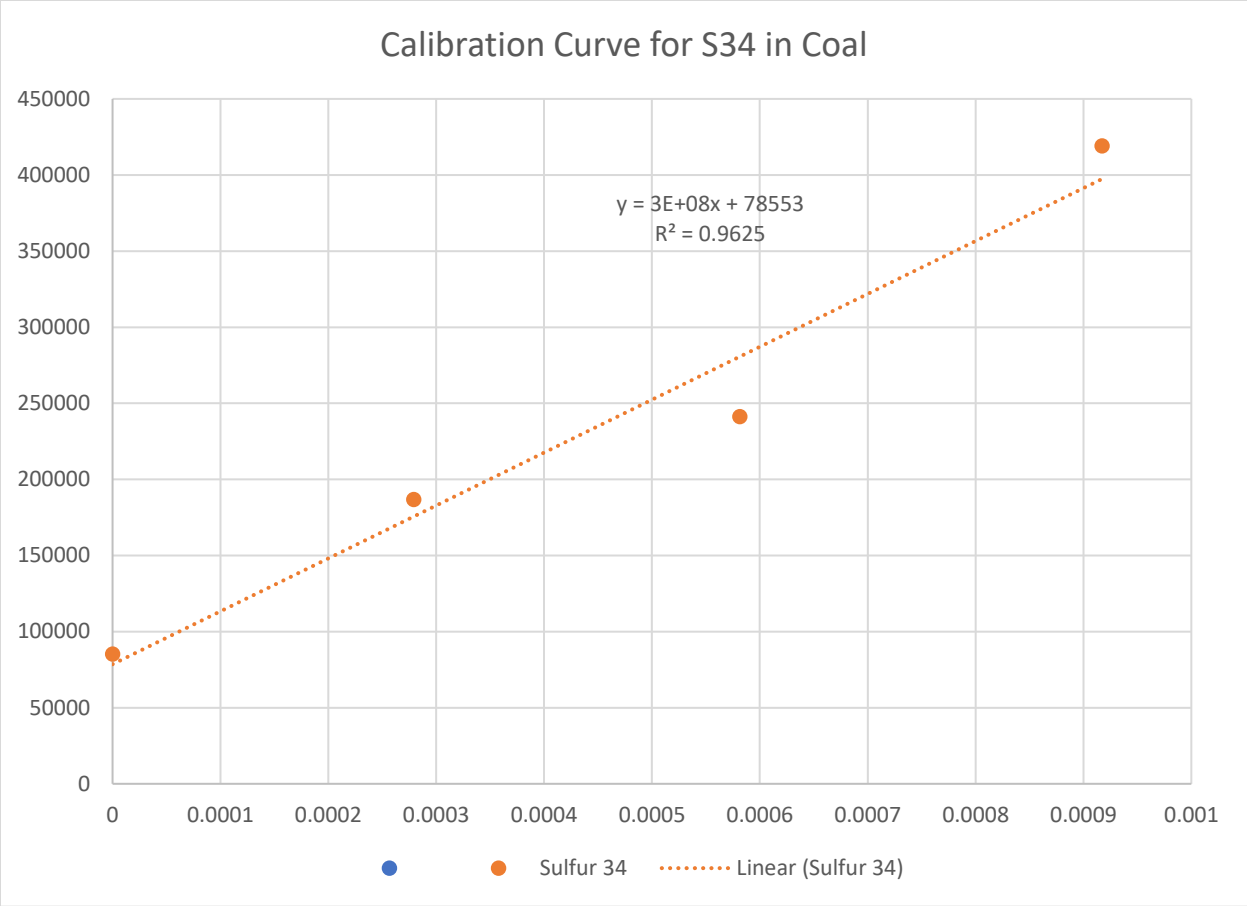

Figure 34. Sulfur Calibration Curve

20191112_124939
(edited - WeVideo).r

Video 1: Video of ICP_MS laser.

Chapter 5. Case Study I – Testing flow ratios and temperatures on bituminous coal

The first test of the proposed technology was done on the bituminous coal. Experiments were performed at various temperatures with CO_2 flow, H_2O flow (hydrothermal), and combined flow (ScWC) in order to asses the effectiveness of supercritical carbon dioxide as solvent and to compare combined flow extraction to more typical hydrothermal extractions. Because fluid characteristics can vary complexly with CO_2-H_2O ratio, a variety of temperatures were explored ranging from 200 – 400 ℃, and sulfur remaining was used as a measure of effectiveness. In our first study, we explored various mixtures and worked to constantly expand our experimental capability, increasing in temperature and flow rate. A master list of all the experiments conducted is given below:

Table 3. Master list of coal extraction experiments conducted.

Experiment	Temperature (°C)	Time (minutes)	Coal (g)	H_2O (g/min)	CO_2 (g/min)	Sulfur (ICP-MS, wt.%)
E120218	200	30	48		5.82	1.13(SL=1.16)
E020519	275	45	49		7.76	1.15
E020619	275	60	50	0.5	5.82	1.03
E022619	275	180	49		7.76	1.06
E032019	275	180	49	0.5	5.82	0.98
E032119	275	180	47	4.99		1.07
E042519	350	60	16		5.82	0.92
E061919	350	60	30	0.5		0.9
E061819	350	60	23		11.64	0.73
E062519	350	60	20	4.99	0.48	0.83
E071019	320	60	18	2.49	11.64	0.74

E072419	290	60	19	2.49		0.71
E072619	290	60	18		11.64	1.01
E081719	350	90	11	3.74	17.46	0.82
E092619	395	135	10		11.64	0.92
E102219	395	120	10	2.49	7.76	0.87(SL=0.83)
E121619	395	120	25	2.49	7.76	1.05
E061220	315	60	10	1.5	0	
E062420	335	60	10	1.5	7.35	
E062520	350	60	10	0	7.35	

The coal mass extracted decreased over time as we came to understand the amount needed for analysis but changes are negligible. The fluid path of our vessel does not directly cross through the loaded solids, so it is likely that the solvent to coal ratios are all higher than necessary. Further testing will be need to understand the mass transfer characteristics in a well design flow path. For the same reason, in the present study, the differences in time are not as important as changes in temperature and fluid composition.

The coal feedstock was analyzed independently by Standard Laboratories using prescribed ASTM methods. The analysis is shown in the Table 2. It showed a 1.14 wt% sulfur content using ASTM D2492. Our in-house ICP-MS analysis gave a similar sulfur content of 1.15 wt.%, but due to high variation, the coal was mixed more thoroughly and a raw value of 1.37 wt% was obtained thereafter. The raw values were assumed to hold constant for all experiments in case study 1, but future experiments have individual raw samples.

Table 4. Analysis of the feedstock coal.

	Dry	***ASTM method***
Ultimate Analysis		
% Nitrogen	1.56	D5373
% Carbon	81.96	D5373

% Hydrogen	4.76	D5373
% Oxygen	4.38	D3176
Total	92.65	
% Moisture		D3302
Proximate Analysis		
Heating value (btu/lb)	14,685	D5865
% Ash	6.20	D3174
% Sulfur	1.14	D4239
% Volatile	25.36	D3175
% Fixed Carbon	68.44	D3172
lbs SO2/MM BTU		
lbs ASH/MM BTU		
Sulfur Forms		
% Sulfate	0.02	D2492
% Pyritic	0.50	D2492
% Organic	0.62	D2492
Total	1.14	
Chlorine (ppm)	1,895	D6721
Mercury (ppm)	0.116	D6722

A total of 17 extraction runs were carried out using the above bituminous coal at a constant pressure of 143 bar with varying extraction time, temperature, water flow rate and CO_2 flow rate, as shown in Table 3. The sulfur content was tracked by ICP-MS analysis in the extracted coal as a measure of extraction effectiveness. Standard Labs results are also presented when available.

Solids recovered after extraction were usually within 2% of the mass loaded after accounting for loss of moisture, except for extractions with pure water at temperatures around 350 °C where about 10% of the mass was lost. The exact masses recovered were difficult to obtain as some coal particles entangled in the glass wool used as filter. In future studies, the glass wool will

be weighed before the experiment and then after collection and drying to assess the change in mass of the coal during extraction.

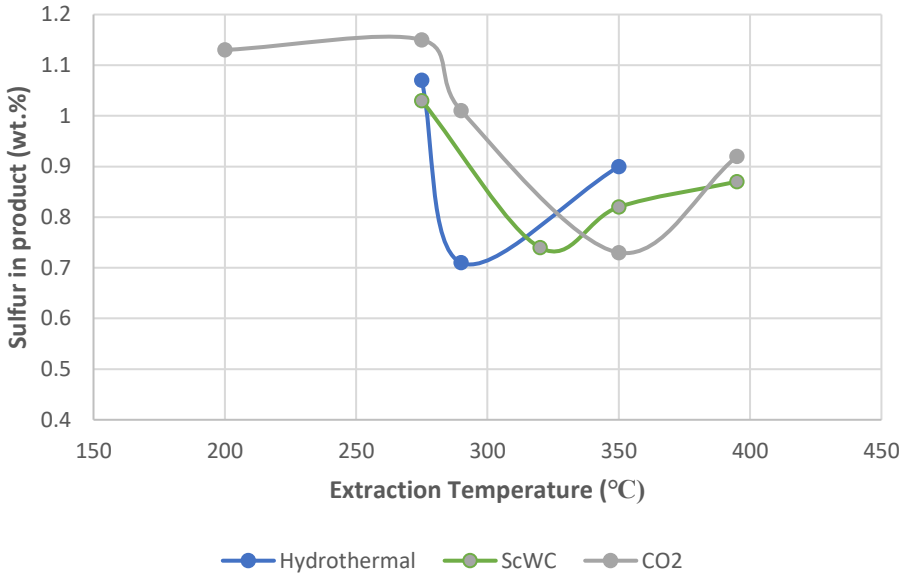

Figure 35: Sulfur remaining in coal after extraction using hydrothermal, ScWC, and CO_2.

Data in Figure 5 shows that carbon dioxide, ScWC, and hydrothermal extraction are all similarly capable of extracting 50% sulfur. Extraction with carbon dioxide was most effective at 350 °C, while extraction with water seemed to be most effective around 300 °C where the ionic concentration was highest. As expected, the hydrothermal extraction was more aggressive at lower temperatures than the carbon dioxide, and the mixture was somewhere in between. Combined flow may provide a synergy that increases extraction but more accurate assessment of the raw coal would be necessary. ScWC, or combined flow, does seem to inhibit organic dissolution that would be expected and was seen from strictly hydrothermal extraction. Although a limited testing was done with flowrate, increasing the flowrate of carbon dioxide extraction at 350°C from 5.82 to 11.64 g/min did result in reducing sulfur content from 0.92 to 0.73 wt.%.

While we studied only a single-step desulfurization reactions, analysis of the sulfur forms indicated that extraction with pure carbon dioxide at 200°C caused pyritic sulfur to be transformed into sulfates that may be easily washed out with warm water. While raw coal contained only 0.02% sulfate and 0.50% pyritic sulfur, E120218 contained 0.16% sulfate and 0.28% pyritic sulfur. In future studies, each extracted mass of coal will be washed with warm water to ensure that the sulfate formed is removed. Sulfur forms analysis was also performed for E061819, the best CO_2 extracted coal. Results showed that the total sulfur content was 0.74 wt%, in excellent accordance with ICP-MS calculated value of 0.73 wt%. The pyritic, sulfate, and organic portions were 0.01, 0.03, and 0.64 wt% respectively. Good conversion of pyrite indicates that the mass transfer from solid to fluid was strong, but the raw level of organic sulfur indicates that organic sulfur was totally inaccessible by CO_2 at 350°C.

In the case of the combined and hydrothermal extractions at 395 °C, the powder coal feedstock turned into a porous-fused mass by a process called hydrothermal carbonization (Figure 6). BET analysis showed that solid product surface area was low, with surface area of 14 m^2/g and average pore radius of 9.9 Å, probably similar to raw coal, which could not be analyzed due to volatile sulfur content. The coal after the extraction at lower temperatures was not fused. Opaque yellow product was typical for all successful extractions.

Figure 36. Products from experiment E102219: coal (left) and dissolved minerals (right)

Ash content was evaluated for the three best extracted coals E061819 (CO2 only), E071019 (ScWC), and E072419 (H2O only). Raw coal was found to have 6.75 % ash, in good accordance with SL data. Neither carbon dioxide nor water seemed to affect the ash content, with E061819 testing at 7.05% and E072419 testing at 6.42%. **ScWC extraction, on the other hand, decreased the ash content to 3.77%, a 45% reduction in ash.**

Extracted coal from E102219 was further sent out for proximate analysis to the Standard Laboratories. The results are compared with the coal feedstock in Table 4. The volatile carbon portion of the raw coal, 25%, had decreased to 12.5% with a corresponding increase in fixed carbon for E102219. Samples E102219 and E062519 both had substantially less carbon ablated during ICP-MS than all other samples. ICP-MS sulfur weight percentages are in accordance with Standard Labs traditional pyrolysis results for selected samples.

Table 5. Proximate analysis of the extracted coal from experiment E102219.

	Raw coal	*Extracted coal from E102219*
Proximate Analysis		
Heating value (btu/lb)	14,685	14,113
% Ash	6.20	6.87
% Sulfur	1.14	0.83
% Volatile	25.36	12.47
% Fixed Carbon	68.44	80.66

Data from ICP-MS analysis of samples from various experiments is given below:

Table 6. Raw data for ICP-MS and calculations.

	S34	s% in pellet	weight S in sample	weight BA	weight coal	S%	C12
raw	379663	0.00086631	0.556	610	32	1.738	55580236
E120218	249136	0.00049078	0.317	612.3	32.9	0.962	58653635
E020519	276598	0.00056979	0.367	612.2	32.6	1.127	83423636
E020619	275009	0.00056521	0.364	612.4	31.7	1.148	83591782
E022619	253500	0.00050333	0.326	615.4	31.7	1.027	92574373
E032019	262214	0.0005284	0.341	613	32.3	1.056	81340120
E032119	253568	0.00050353	0.325	612.7	33.2	0.980	67879826
E041519	264713	0.00053559	0.345	612.2	32.4	1.066	77845157
E042519	394277	0.00090835	0.583	610	32	1.822	73909796
E061919	234151	0.00044766	0.291	618.9	31.6	0.922	45117301
E061819	236968	0.00045577	0.296	615.9	32.8	0.901	66625854
E062519	205650	0.00036567	0.238	618.9	32.7	0.729	67698660
E070319	148980	0.00020262	0.132	616.4	32.9	0.400	33220007
E071019	248253	0.00048824	0.313	610	32	0.980	57201793
E072419	207111	0.00036987	0.237	610	32	0.742	62240067
E072619	201929	0.00035496	0.228	610	32	0.712	65710217
E080219	253254	0.00050262	0.323	610	32	1.008	61920240

E081719	220408	0.00040812	0.262	610	32	0.819	57833318
E092619	237411	0.00045704	0.293	610	32	0.917	70176848
E102219	139500	0.00017535	0.113	610	32	0.352	28014785
E121619	255348	0.00050865	0.328	614.2	31.3	1.049	73768502

Observing low carbon 12 counts seems to be a way to assess whether or not the coal has carbonized. The more graphitic carbon is more resistant to laser ablation.

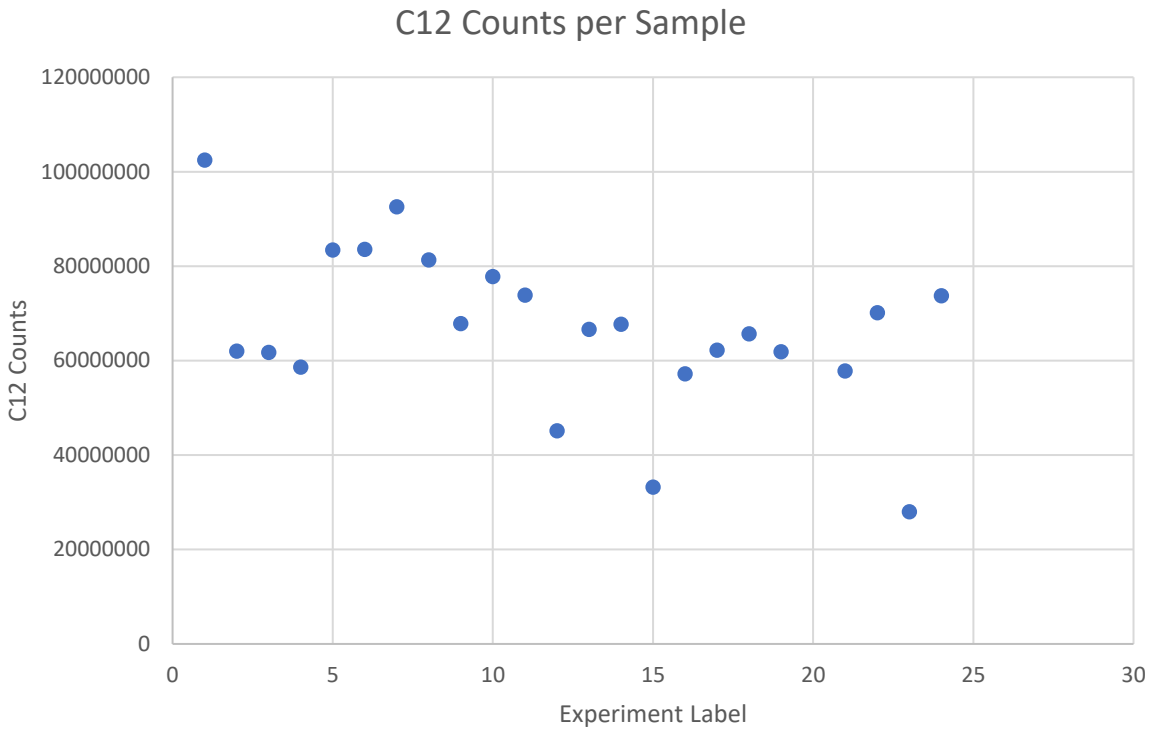

Figure 37: C12 Counts for extracted coal from various experiments

The first four experiments are standards, and afterword, the amount of carbon ablated is fairly consistent, with three exceptions: experiment E042519(label 12), E070319 (label 15), and E102219 (label 23). All three had water that became supercritical as the experiment was shutdown or during operation. In a supercritical state the polarity of the fluid will be very low and the carbon framework may be affected. Surprisingly though, E042519 seemed to experience

some carbonization despite not having any water present during the experiment. Furthermore, carbonization was not noted during the extraction of coal with carbon dioxide at higher temperature in experiment E092619. Experiments after E042519 were cooled with low pressure carbon dioxide flow in order to prevent the vessel from overheating at the beginning of shutdown, when the low enthalpy fluid inlet is stopped. Therefore, carbonization of our coal seems to occur in CO_2 near 350 ℃, and in water above 375℃, and may prefer natural cooling as opposed to forced cooling.

The sulfur counts were first converted to sulfur value for the pellet using the calibration curve created. Next the overall weight of sulfur in the pellet would be calculated using the specific weight of the pellet formulated. From the overall weight of sulfur in the pellet the overall weight of sulfur in the coal was determined by assuming no sulfur was present in the filler, which was boric acid. Because some samples were resistant to ablation due to carbonization, the sulfur value was scaled up by the ratio of the typical carbon ablated divided by the specific carbon ablated. Typical counts for carbon were about 70,000,000 so E070319 and E102219 were scaled by 2.08 and 2.47 to values of 0.83 and 0.87 wt% sulfur, which correspond well with independent analysis

To further understand the characteristics of the extracted coal from E102219 experiment, x-ray diffraction and thermo-gravimetric analyses were carried out and the results are compared to raw coal.

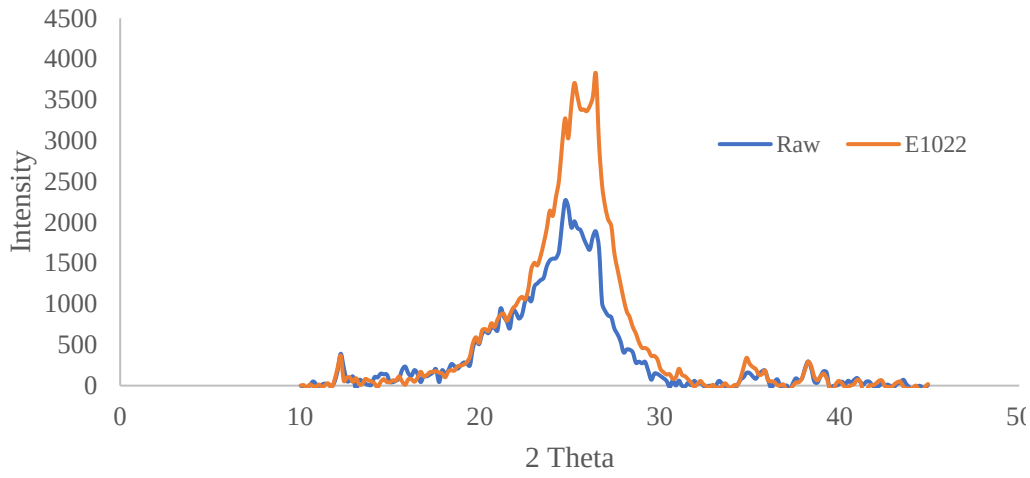

Figure 38. X-ray diffraction analysis (left) and thermo-gravimetric analysis (right) of the extracted (E102219) and raw coals.

XRD spectra for coal contain two main peaks for carbon at 2θ of 25° and 26.5°. Raw coal has a more prominent peak at 25° with a smaller peak at 26.5°. For E102219, the higher intensity indicates a more ordered crystalline structure as compared to raw coal. Also, the peak at 26.5° has become larger than the peak at 25°. The 26.5° peak is associated with synthetic graphite, and the peak at 25° can be attributed to carbon that is not graphitic.

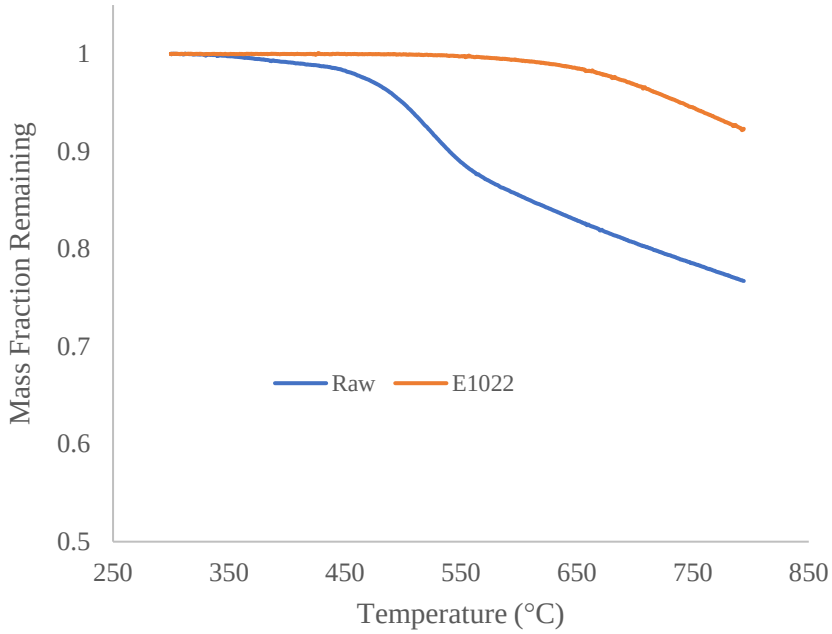

Figure 39: TGA of raw and E1022

Thermogravimetric analysis was carried out in nitrogen atmosphere and shows the difference in volatility between raw and extracted coal. By 800 ℃, the raw sample has lost 23.2% of mass, compared to only 7.7% mass for E1022. Although we extracted only to 395℃, E102219 is considerably less volatile in the range of 400 - 800℃.

Raman spectra for raw sample have higher counts and a more angled baseline due to fluorescence of metals contained in the raw coal (Figure 8). This fluorescence is not noticed in the extracted sample from E102219, which has a nearly flat baseline and lower noise, indicating a lack of fluorescence generating metals. Two characteristic carbon peaks appear at 1350 and 1600 cm^{-1}. With baseline subtracted, the peak heights and ratios are the same. A slight broadening of the peak at 1350 cm^{-1} is noticeable with two shoulder peaks becoming more prominent.

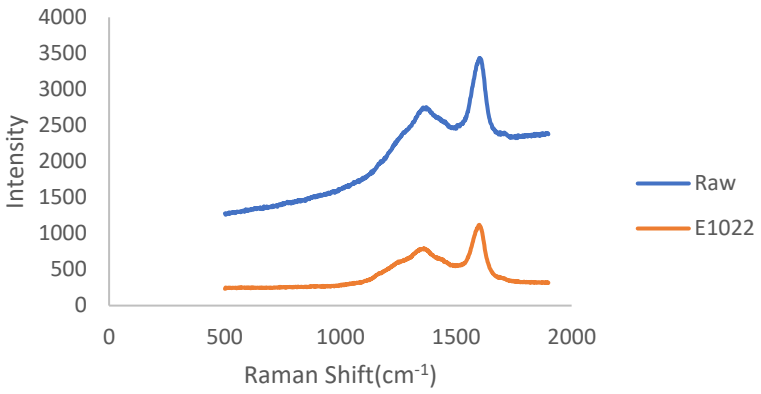

Figure 40: Raman shift spectra for raw coal and the extracted coal from E102219.

Thus, the extraction with fluid above the supercritical point of pure water (375°C) caused hydrothermal carbonization which may be useful for further upgrading carbon once the heteroatoms have been extracted at temperatures between 300-350°C. The presence of carbon dioxide during hydrothermal carbonization may cause volatile carbon content to crosslink in the solid instead of being extracted by the solution. From the proximate analysis, E102219 has retained most of its heating value. Removing the sulfur should decrease the heating value slightly, but crosslinking volatile carbon into fixed carbon would increase the heating value. Importantly, the combined extraction seems to crosslink carbons that would be extracted and lost by hydrothermal extraction.

5.1 Key Scientific Observations

1. Can high enthalpy carbon dioxide be oxidative enough to react with pyritic or organic sulfur in coal?

   Yes, carbon dioxide and sulfur will react to form carbon monoxide and sulfur dioxide. Under carbon dioxide pressure, coal was confirmed to have undergone

sulfur loss not explainable by thermal treatment alone. While it has been known from combustion research that carbon monoxide exists in small quantities in equilibrium with carbon dioxide at high temperatures, never has the use of carbon dioxide as an oxidizing agent been reported. Because carbon dioxide becomes supercritical at such a low and manageable temperature, little work is done to study it at high temperature. We were impelled by the question: can we use this abundantly available waste product carbon dioxide to perform value added extraction on raw coal with waste levels of power plant heat?

2. How does the CO_2-H_2O mixture behave in terms of ionization of various components?

   Water may ionize into hydronium and hydroxide ions according to the ionization constant of water that peaks around 325°C. First and second ionization of carbonic acid will be strongest at lower temperature, and decrease with increasing temperature. Carbonate and hydroxide ions should play a role in extraction as well as the hydronium ions.

3. What is the fate of various forms of sulfurs in the coal in CO_2-H_2O atmosphere?

   Sulfur can evolve to form elemental sulfur, sulfur dioxide, and hydrogen sulfide. With CO2 extraction, no liquid extract is collected and the effluent vapor smells strongly of burnt matches, indicating that sulfur dioxide is formed exclusively in CO2. Extracting with only water, the liquid extract seems to smell of rotten eggs, indicative of hydrogen sulfide. Both sulfur dioxide and hydrogen sulfide have boiling points below 0°C, and any sulfur in the liquid effluent seems to evaporate or react with other components to form an ash that settles from the extract. From

literature, elemental sulfur is created during the formation of hydrogen sulfide but not sulfur dioxide. The strong yellow color of aqueous extracts compared to lack of yellow residue after CO2 extraction supports the hypothesis that water promoted formation of hydrogen sulfide and elemental sulfur, while carbon dioxide promoted formation of sulfur dioxide. Experimentally measuring sulfur values would require FTIR analysis of gas products.

4. What are the reaction kinetics of organic and inorganic sulfurs in CO_2-H_2O atmosphere?

   From E071019, we can say that 50% of total sulfur is removed in one hour. For 18 grams of coal, 205 mg of sulfur was reduced to 100 mg. Thus about 100 mg total sulfur per hour were extracted. Our vessel though was designed for synthesis and the flowrate does not directly impinge on the solids, so kinetic values provided by this study are insufficient for scaleup.

5. Is there is an optimum CO_2-H_2O ratio and temperature profile that can remove sulfur but keep carbon?

   Extraction below 350℃ is best for sulfur removal efficiency. With water, the polarity begins to decline too much even before 350℃. The Virginia coal that we tested did not seem to be susceptible to organic dissolution as other coals undergoing hydrothermal treatment have been. Surprisingly, extraction at higher temperatures resulted in carbonization, whereby the volatile carbon in the coal became fixed carbon.

6. What is impact of the extraction time and flowrate on removal efficiency?

   Although our vessel is not well equipped to study mass transport, we did notice increases in extraction efficiency when increasing flowrate such as increasing the

flowrate of carbon dioxide extraction at 350℃ from 5.82 to 11.64 g/min resulting in a reduced sulfur content from 0.92 to 0.73 wt.%. At 275 ℃ and 390℃, extractions for longer times did not seem to increase extractive efficiency as compared to the negative effect that poor temperature range had.

7. How does the ash content in the coal change upon extraction?

   ScWC decreased ash content by 45% as opposed to no change from hydrothermal or carbon dioxide extractions alone, according to ash content results for coals E061819, E071019, and E072419. Carbon dioxide alone should not be expected to remove ash, but the hydrothermal treatment has been effective at extracting even heavy metals in literature. Although hydrothermal method is often effective with ash removal, our coal was resistant to hydrothermal ash extraction without the added effect of the carbon dioxide ions.

8. What is the impact of the extraction treatment on the flow-ability of the cleaned coal?

   To use an extraction tower with automated semi-continuous hopper feed, the coal should not be allowed to carbonize so that coal flows smoothly into the combustion unit. To this end, the temperature should be kept lower than 350℃, which is where sulfur extraction efficiency is higher anyway. Controlling the cooling rate of the coal after extraction may also be an effective way to prevent carbonization and thus clogging.

9. How does the particle size and surface area influence the kinetics?

   We were not able to study different particle sizes, but decreasing the particle size will increase the extraction efficiency by increasing mass transport capability.

Getting below the crushed size that we use would require more energy intensive grinding whose cost would start to rival the marginal benefit of faster kinetics.

Chapter 6. Case Study II - Adding ultrasound energy to improve extraction of Bituminous Coal

Ultrasound waves can be added to solution to enhance the mass transport of the fluid. A piezoelectric crystal is attached to a horn that is placed in the vessel near the solids. Crystals may also by placed on the exterior of vessels after some calculation, but thick steel will dampen ultrasound waves. Traditionally, the formation of bubbles leads to increased mixing and increased ion activity caused by the collapse of the bubbles. In supercritical solution though, two phases cannot exist and bubbles will not form. Still, the addition of pulsed ultrasound waves are expected to further increase the mixing and mass transport of the supercritical fluid which may be important for penetrating the solid matrix of coal. Most ultrasound studies focus on the use of basic hydroxide solutions that enhance the formation of hydrogen peroxide, which performs the critical steps in chemical extraction of sulfur and ash.

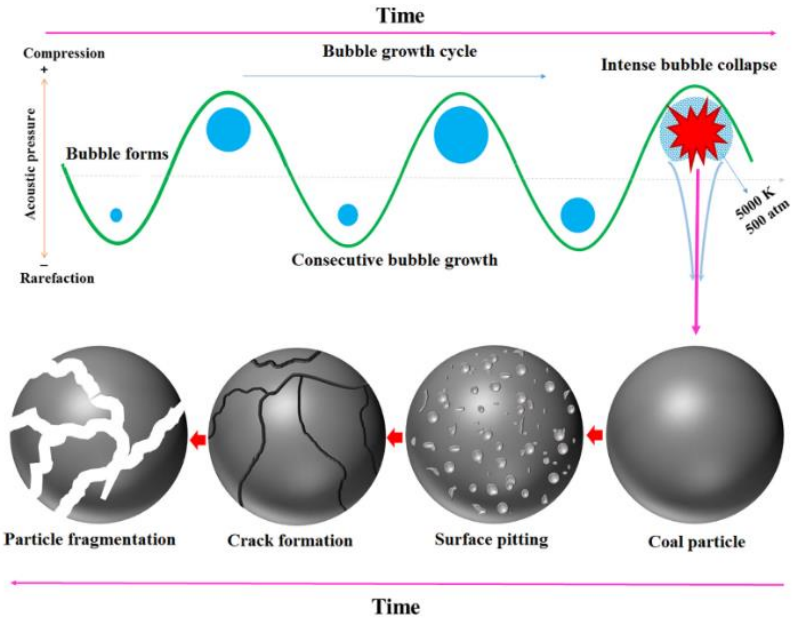

Figure 41: Bubble formation and collapse caused by ultrasound waves. (Barma 2019)

Study is ased on experiments E061220, E062420, and E062520 which are all run for one hour at optimum temperature for the given fluid mixture on 10 grams of coal. E061220 was run with only water at 315℃, E062420 was run with combined flow at 335℃, and E062520 was run with only CO2 at 350℃. The mass of the glass wool filter is measured before the experiment and after collecting and drying so that the mass of the coal recovered is now accurate enough to calculate the organic dissolution. In addition, individual raw samples were collected instead of assuming a flat raw value. Coal was also washed after extraction with 90 ℃ water to remove any sulfur that had been oxidized to sulfate form. Samples will be ground, pelletized, and analyzed by ICPMS and for ash content using the tube furnace.

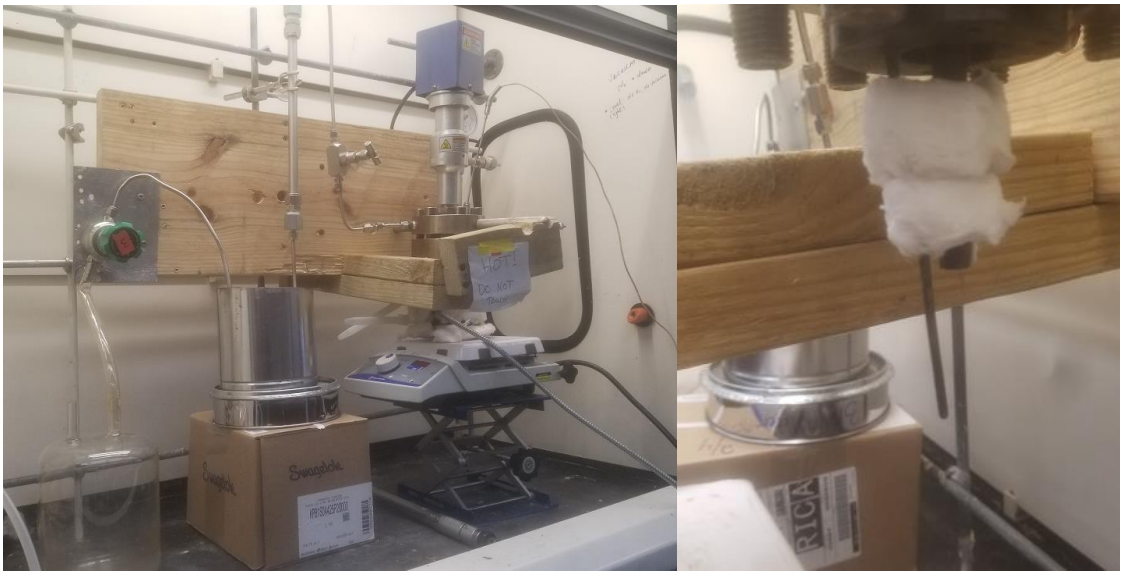

Figure 4212: (Left) Exterior of extraction setup used with sonication horn indicated. (Right) Sonication horn on the interior of the vessel to be in contact with fluid and solids.

Experiments were performed successfully at 2100 psi without leaks. Ultrasound energy was pulsed for one second on, one second off at 120 Watts. An aututuner keeps frequency between 20-25 kHz. An increase in temperature was noticed when ultrasound was turned on, but the temperature controller effectively kept temperature at the experiment setpoint. After accounting for coal collected in the glass filter, organic dissolution could be approximated. The

mass of coal collected after extraction and drying for E061220, E062420, and E062520 were 9.32, 8.74, and 8.55 grams. Thus, organic dissolution did not seem to occur appreciably for hydrothermal treatment as compared to CO_2 treatment or combined flow.

Ash content analysis indicates that the extractions with ultrasound were not particularly effective. All three extracted samples seemed to test at levels equal to raw coal. For E061220, E062420, and E062520 – 8.38, 8.30, and 7.66% ash. With more vigorous mixing the ash content of later samples was a bit higher (around 8%) than earlier studied raw (around 6.5%). There is also a possibility that some of the glass wool may have broken off and/or dissolved followed by precipitated on solid coal. This could increase the ash content of the coal.

ICP-MS also indicated that samples were not extracted in terms of the sulfur content. Raw sample had sulfur counts of 256,000 compared to 230,000 for water only 211,000 for combined flow and 199,000 for only CO2, corresponding to 1.08 wt% sulfur still remaining in the extracted sample.

The increased energy from the ultrasound decreased effectiveness compared to runs without ultrasound at the same temperature. This decrease in extraction can probably be explained by a critical decrease in fluid density. Although the mixtures were still supercritical, they behaved more like gases due to the increase in energy and mixing from the ultrasound pulses. The carbon dioxide was less affected and produced the best results with ultrasound because the carbon dioxide is already well superheated and increases in the fluid enthalpy will no longer result in drastic change to density.

In future work, the ultrasound should be tested below 300 ℃ to discover if the coal can be extracted with higher solvent and thermal efficiency compared to higher temperature without ultrasound.

Chapter 7. Industrial Applications

The technology developed in this work can potential contribute to the energy industry in a variety of way in addressing current challenges. Some of the applications are summarized below:

Reduction in the emission of pollutants

The proposed supercritical water-carbon dioxide (ScWC) extraction technology has potential to help industry in mitigating hazardous aerosol pollutant emission by reducing the need to treat flue gas and increasing the use of flue gas streams for energy recovery. Successfully removing sulfur and other hazardous molecules from the raw coal before combustion would eliminate/reduce pollution of ash, limestone slurry, and air. While many post combustion efforts prove to trade one form of pollution for another, our proposed pre-combustion extraction process seeks to reduce waste in all three phases. In the traditional combustion, treating the flue gas instead of raw coal results in a substantial volume of gas to be processed. This also hinders the ability to further harvest thermal energy from the stream; small improvements in the thermal efficiency of large power plants can have drastic overall economic effects. Pollutant-free flue gas stream may also allow for direct compression of carbon dioxide for sequestration and use. The presence of sulfur and mercury is the main reason for coal processing for power generation to become an expensive proposition. Removing them pre-combustion also offers the potential to use coal for other beneficiated products where these two elements are not desired in the products. The use of CO_2 and H_2O mixture has potential for industrial applications in power plants as both CO_2 and H_2O are available on site. The proposed process has potential to provide new synergy with Brayton cycle power generation, oxyfuel combustion, biomass cofiring, and enhanced oil recovery technologies or sequestration.

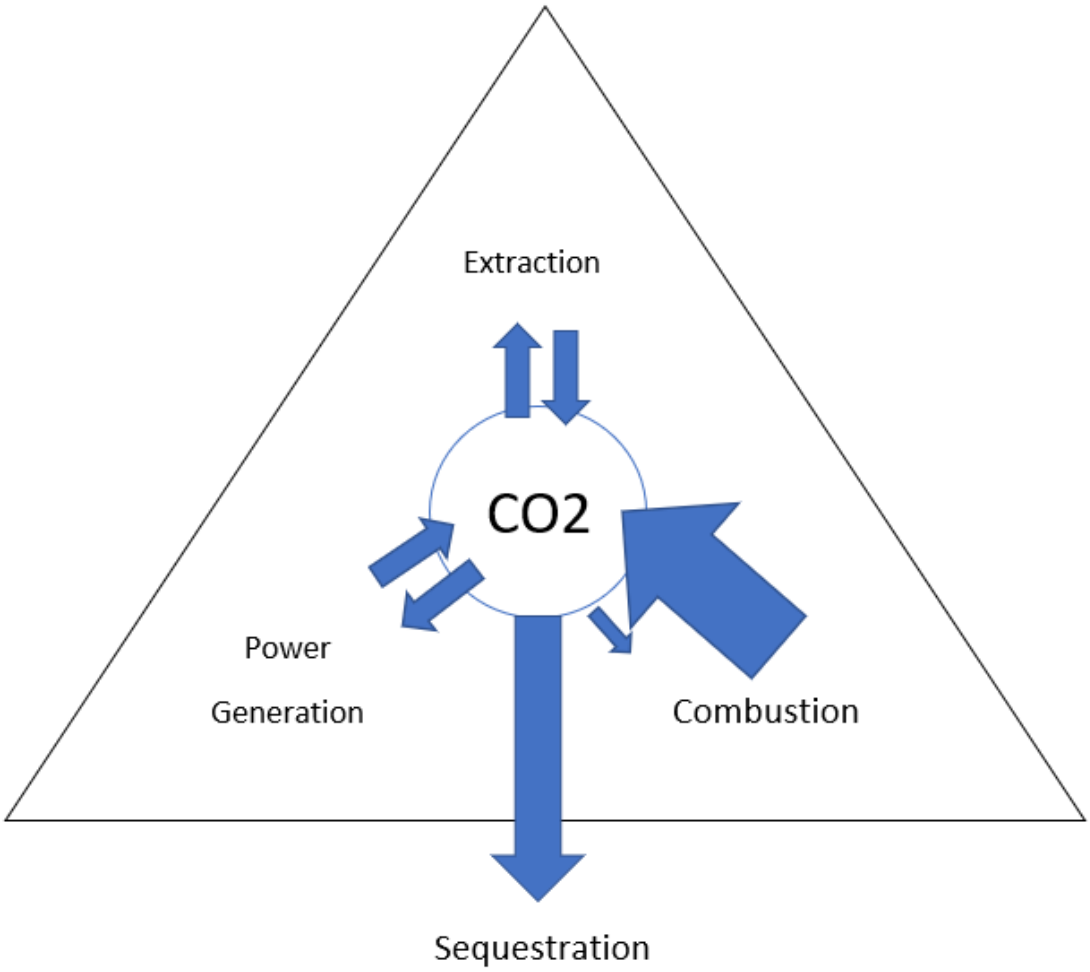

Figure 43: Carbon Dioxide Process Synergy for Clean Coal Fired Electricity Production

Increase in the power production efficiency

To avoid the substantial volume of nitrogen to be separated from the combustion exhaust, oxyfuel combustion could be used whereby the inlet air is separated into pure nitrogen and oxygen with a cryogenic separations unit. Without the volume of nitrogen, carbon dioxide as a diluent would also be fed to the combustion unit in order to control the combustion composition-envelope and temperature of combustion. Without nitrogen to separate, the combustion effluent will be a high percentage carbon dioxide with some water.

The power generation unit could incorporate Brayton cycles where carbon dioxide is used as the working fluid instead of water. These plants have been in development for some time as a next generation technology aiming for several percentage points in thermal energy efficiency at large scale power plants. The power generation unit, like the extraction unit, will not consume carbon dioxide but rather use it as a working fluid.

The extraction unit would involve one large solid-supercritical fluid extraction tower with hoppers for loading and unloading. The extraction effluent containing sulfur and metals would then be used in a pressure fractionation scheme using the water, carbon dioxide, and entrainers to condense out elements from high mass to low mass in sequential flash tanks. Heavier metals in aqueous suspension would be produced by relieving a small amount of enthalpy from the effluent in the first flash tank, while lighter metals would remain dissolved and travel with the vapor to the next flash tank. The pressure and temperature of the flash tanks can be set according to the number of tanks possible or the desired separation. In this way, valuable and scarce heavy metals can be targeted and concentrated instead of accumulating in ash piles. Carbon dioxide would be cleaned of sulfur and regenerated through a process like the Claus process, whereby vaporous sulfur is burned to form solid elemental sulfur and the heat recycled.

Recovery of rare earth elements

Rare earth elements are heavy metals that are used in small quantities in the construction of advanced technological devices. The U.S. and the world have long relied on China for rare earth elements due to a heavily concentrated mud pile in China. Recent discovery of another trove in Japan was announced in 2012, but the site is far underground and will take some years to produce. China even has the ability to use these rare elements in trade wars, as the production is not economical at the lower concentrations of the same element mixes found in coal. Carboxyhydrothermal processing may provide the U.S. with the ability to access and concentrate the vast stores of rare earth elements seen as waste in coal ash piles.

Upgradation of biomass for use in power plants

Due to the flexibility of design with temperature and flow ratio, the carboxyhydrothermal extraction could handle various ranks of feedstock. The process would also be useful for upgrading lower grade biomass for cofiring. Often these biomass feedstocks have high amounts of ash that can destabilize the combustion parameters, so only a small portion can be added. Despite low calorific value compared to hydrocarbons, biomass waste cofiring is beginning to be mandated in order to improve sustainability. The proposed extraction would be able to demineralize biomass sources to the necessary degree, and then add value to the biomass through hydrothermal carbonization.

Having these technologies work together will create synergy through the collective handling of carbon dioxide and cost-effective separation, but most importantly; carbon dioxide handling will allow for sequestration instead of release to the atmosphere. Because carbon

dioxide is actually in such small concentration in the exhaust of traditional combustion schemes, the carbon dioxide cannot be captured and sequestered. In this scheme, the whole combustion is reimagined so that the end result is a clean, pumpable carbon dioxide. That carbon dioxide can then be sequestered into the ocean and old liquid hydrocarbon wells, or even used in active wells as a replacement for fracking chemicals. One such oil recovery scheme built in Texas, the Petra Nova project, boasts a 1300% increase in oil production, over a million tons of captured carbon dioxide per year, and zero carbon dioxide escape.

Chapter 8. Conclusions

Supercritical water-CO_2 (ScWC) and supercritical CO_2 extractions are proposed for cleaning of coal before combustion. Coal beneficiation is demonstrated in 200-400 ^oC range at 143 bar using a semi-continuous process without needing any mineral acid or organic solvents by studying the sulfur removal. A high pressure chemical reactor scheme was developed in order to perform extractions. An accurate ICP-MS technique was developed to quickly track sulfur removal of our process.

Carbon dioxide extraction at 350 ℃ is effective similar to the typical hydrothermal extraction which was most effective at 290℃. Extraction with carbon dioxide caused more difficult-to-remove pyritic and organic sulfurs to become sulfate by 200℃. Extracted solids contained about 50% less sulfur than raw coal for 1-hour extractions using CO_2 at 350 ℃, water at 290 ℃ or combined H_2O-CO_2 at 320 ℃. Thus, the extractive strength of the fluid can be tuned by adjusting the temperature and H_2O/CO_2 flow ratio. Furthermore, the ash content was considerably affected by ScWC extraction, with combined extraction producing 50% ash reduction in one hour.

We demonstrated a new reaction of sulfur with carbon dioxide whereby carbon dioxide is used to donate oxygen atoms to a solid matrix in forming carbon monoxide. This reaction is similar to previous reaction studied with nitric acid whereby elemental sulfur and sulfur dioxide are produced. Expensive organic solvent, then, may be replaced by use of an abundant waste product.

In studying the mass transport of the fluids, we found that adding ultrasound did not increase the effectiveness of extraction at previous optimized temperatures. While the carbon dioxide extracted sample still contained 50% sulfur, the pyritic sulfur was almost completely reacted and the organic portion was completely unreacted. This indicates that the mass transport

into the coal matrix was already good, but the temperature was not sufficient to target the organic sulfur bond at all.

Extraction with pure water above the supercritical point of pure water caused hydrothermal carbonization of coal solids where volatile carbons were crosslinked into fixed carbons. Some carbonization occurred even with strictly carbon dioxide extraction. Previous reports of carbonization convert a biomass waste into a low rank coal, but here we show that carbonization can occur at higher temperatures to produce higher rank coals from middle rank coals. Carbonization caused the coal mass to fuse upon drying and may be interesting for further carbon upgrading, but should be avoided for coal meant to be combusted. Hence, it is preferable to operate at 320 ^{o}C or below to obtain a free-flowing extracted coal.

These studies provide several meaningful scientific discoveries in the area of thermodynamic solution manipulation and extraction for biomass conversion and beneficiation. Despite answering several important questions, many new questions have arisen that should be studied in future work.

Chapter 9. Suggested Future Research

To further developed the proposed technology, following future work is proposed:

Case Study III – Test ScWC for high sulfur coal

The technology should be further tested if high sulfur coal can be treated. If successful, the ScWC can help reduce the environmental pollution in many countries that rely on high sulfure coal. One example is high sulfur coals in India and China which are rapidly expanding their coal use. The high sulfur content coal (~4%) can be studied using the combined flow technique. Coal should be loaded into a reactor extension that allows for more direct fluid-solid contact than loading into the reactor vessel. Coal should be extracted for 1, 3, and 6 hours with combined flow at 335 ℃. The temperature may be set at 355℃ to account for cooling between the vessel and the extension. The organic dissolution, sulfur forms, TGA, and ash content should be studied as previously for the ultrasound experiment.

Case Study IV – Test ScWC to produce ultra-clean coal and coke

The ScWC has potential to produce ultra-clean coal and coke from the low-sulfur coals in the United States. The product can then have high value applications in the metals and batteries industries. The bituminous coal should be loaded into the vessel extension and extracted for 8 hours with combined flow at 335℃. The coal should then be unloaded, and washed. A small portion should be removed for analysis. The extracted coal should then be added to the reactor vessel and hydrothermally carbonized at 400℃ for 48 hours. Step one should produce a fairly clean coal, and step two should increase the value of the carbon structure. Ash and sulfur should be studied with the tube furnace and ICP-MS, and the carbon content will be studied using XRD, TGA, RAMAN, and heating value will be measured by Standard Labs.

Case Study V – Fundamental probing of the mechanism

Carbonization should be studied to discover if any organic sulfur is removed in the process. Though a rough idea is gained from this work, separate reaction rates should more closely be studied for pyrite, organic sulfur, and ash. Ultrasound should be studied with lower temperatures and its effect on reaction rates. For scaleup, many considerations concerning the regeneration and separation of clean CO_2 should be studied. The necessary input purity for carbon dioxide extraction should be explored, as only supercritical fluid grade was used here to ensure good operation of lab scale pumps.

Chapter 10. References

Akers, D. J. (1996). Coal cleaning controls HAP emissions. *Power Engineering*, *100*(6), 33-37.
Ambedkar B, Nagarajan R, Jayanti S (2011) Ultrasonic coal-wash for de-sulfurization. Ultrasonic Sonochemistry 18:718-726.

Allaf, T., Tomao, V., Ruiz, K., & Chemat, F. (2013). Instant controlled pressure drop technology and ultrasound assisted extraction for sequential extraction of essential oil and antioxidants. *Ultrasonics Sonochemistry*, *20*(1), 239-246.

Baláž P, LaCount RB, Kern DG (2001) Chemical treatment of coal by grinding and aqueous caustic leaching. Fuel 80:665-671.

Barma, Santosh Deb. "Ultrasonic-assisted coal beneficiation: A review." Ultrasonics sonochemistry 50 (2019): 15-35

Belošević, S. V., Tomanović, I. D., Crnomarković, N. Đ., & Milićević, A. R. (2017). Modeling of pulverized coal combustion for in-furnace NOx reduction and flame control. *Thermal Science*, *21*(suppl. 3), 597-615.

Berka-Zougali, B., Hassani, A., Besombes, C., & Allaf, K. (2010). Extraction of essential oils from Algerian myrtle leaves using instant controlled pressure drop technology. *Journal of chromatography A*, *1217*(40), 6134-6142.

BP (British Petroleum) 2011 Statistical Review of World Energy; June 2012. Accessed 24 June 2020

Baruah, B. P., & Khare, P. (2007). Pyrolysis of high sulfur Indian coals. *Energy & Fuels*, *21*(6), 3346-3352.

Baruah, B. P., & Khare, P. (2010). Mobility of trace and potentially harmful elements in the environment from high sulfur Indian coal mines. *Applied Geochemistry*, *25*(11), 1621-1631.

BP (British Petroleum) 2019 Statistical Review of World Energy; June 2020. Accessed 24 June 2020 URL https://ourworldindata.org/grapher/coal-consumption-by-region

Calkins, W. H. (1994). The chemical forms of sulfur in coal: a review. *Fuel*, *73*(4), 475-484.

Chabukdhara, M., & Singh, O. P. (2016). Coal mining in northeast India: an overview of environmental issues and treatment approaches. *International Journal of Coal Science & Technology*, *3*(2), 87-96.

Conrad, Jacy, Swaroop Sasidharanpillai, and Peter R. Tremaine. "Second Dissociation Constant of Carbonic Acid in H2O and D2O from 150 to 325° C at p= 21 MPa Using Raman Spectroscopy and a Sapphire-Windowed Flow Cell." The Journal of Physical Chemistry B 124.13 (2020): 2600-2617.

Dai, S., Graham, I. T., & Ward, C. R. (2016). A review of anomalous rare earth elements and yttrium in coal. *International journal of coal geology*, *159*, 82-95.

Davidson, R. M. (1994). Quantifying organic sulfur in coal: A review. *Fuel*, *73*(7), 988-1005.

De Gouw, J. A., Parrish, D. D., Frost, G. J., & Trainer, M. (2014). Reduced emissions of CO2, NOx, and SO2 from US power plants owing to switch from coal to natural gas with combined cycle technology. *Earth's Future*, *2*(2), 75-82.

Ding L, Gao Y, Li X et al (2019) A novel CO2-water leaching method for AAEM removal from Zhundong coal. Fuel 237:786-792.

Energy Information Agency (2018) International Energy Outlook 2017 https://www.eia.gov/todayinenergy/detail.php?id=37293. Accessed 21 March 2020

El-Midany AA, Abdel-Khalek MA (2014) Reducing sulfur and ash from coal using Bacillus subtilis and Paenibacillus polymyxa. Fuel 115:589-595.

2018 Electric Power Annual U.S. Energy Information Administration, Accessed 24 June 2020

Fleig, D., Andersson, K., Johnsson, F., & Leckner, B. (2011). Conversion of sulfur during pulverized oxy-coal combustion. Energy & Fuels, 25(2), 647-655.

Flett, D. S., & Melling, J. (1979). Extraction of ammonia by commercial copper chelating extractants. *Hydrometallurgy*, *4*(2), 135-146.

Funke, Axel, and Felix Ziegler. "Hydrothermal carbonization of biomass: a summary and discussion of chemical mechanisms for process engineering." Biofuels, Bioproducts and Biorefining 4.2 (2010): 160-177

Gabler Jr, R. C., & Stoll, R. L. (1982). Extraction of leachable metals and recovery of alumina from utility coal ash. *Resources and conservation*, *9*, 131-142.
Gao Y, Ding L, Li X et al (2017) Na&Ca removal from Zhundong coal by a novel CO2-water leaching method and the ashing behavior of the leached coal. Fuel 210:8-14.

Gupta, J. (2010). A history of international climate change policy. *Wiley Interdisciplinary Reviews: Climate Change*, *1*(5), 636-653.

Gupta RB (2005) Supercritical Water Oxidation. Encyclopedia of Chemical Processing, Marcel Dekker.

He, J., Tan, M., Zhu, R., & Luo, Z. (2016). Dry beneficiation and cleaning of Chinese high-ash coarse coal utilizing a dense-medium gas-solid fluidized bed separator. *Physicochemical Problems of Mineral Processing*, *52*.

Humphries, M. (2010). *Rare earth elements: the global supply chain*. Diane Publishing.
June 2020 Monthly Energy Review, U.S. Energy Information Administration, Accessed 24 June 2020

IDE, S., OHKI, A., & TAKAGI, M. (1985). Diphosphonium-type liquid anion-exchange extractants. Extraction of anionic metal complexes. *Analytical sciences*, *1*(4), 349-354.

Kabyemela BM, Adschiri T, Malaluan RM and Arai K, Glucose and fructose decom position in subcritical and supercritical water: detailed reaction pathway, mechanisms, and kinetics. Ind Eng Chem Res 38:2888–2895 (1999).

Ken, B. S., & Nandi, B. K. (2019). Desulfurization of high sulfur Indian coal by oil agglomeration using Linseed oil. *Powder Technology*, *342*, 690-697.

Kritzer, P.; Dinjus, E. An assessment of supercritical water oxidation (SWO). Existing problems, possible solutions and new reactor concepts. Chemical Engineering Journal (2001), 83(3), 207-214.

Lin, R., Howard, B. H., Roth, E. A., Bank, T. L., Granite, E. J., & Soong, Y. (2017). Enrichment of rare earth elements from coal and coal by-products by physical separations. *Fuel*, *200*, 506-520.

Meshram, Pratima, et al. "Demineralization of low grade coal–A review." *Renewable and Sustainable Energy Reviews* 41 (2015): 745-761.

Mketo N, Nomngongo PN, Ngila, JC (2016) Evaluation of different microwave-assisted dilute acid extracting reagents on simultaneous coal desulphurization and demineralization. Fuel 163: 189-195.

Mooiman, M. B., & Miller, J. D. (1991). The chemistry of gold solvent extraction from alkaline cyanide solution by solvating extractants. *Hydrometallurgy*, *27*(1), 29-46.

Morimoto M, Nakagawa H, Miura K (2008) Hydrothermal extraction and hydrothermal gasification process for brown coal conversion. Fuel 87:546-551.

Nelson DA, Molton PM, Russell JA and THR, Application of direct thermal liquefaction for the conversion of cellulosic biomass. Ind Eng Chem Prod Res Dev 23:471–475 (1984).

Odetayo, B., Kazemi, M., MacCormack, J., Rosehart, W. D., Zareipour, H., & Seifi, A. R. (2018). A chance constrained programming approach to the integrated planning of electric power generation, natural gas network and storage. *IEEE Transactions on Power Systems*, *33*(6), 6883-6893.

Pollet, B. G., Staffell, I., & Adamson, K. A. (2015). Current energy landscape in the Republic of South Africa. *International Journal of Hydrogen Energy*, *40*(46), 16685-16701.

Qian, J., Zheng, H., Song, Y., Wang, Z., & Ji, X. (2008). Special Properties of Fly Ash and Slag of Fluidized Bed Coal Combustion [J]. *Journal of the Chinese ceramic society*, *10*.

Qiu, X. C., & Zhu, Y. Q. (1993). Rapid analysis of cation exchange properties in acidic soils. *Soil science*, *155*(4), 301.

Rivera, N., Hesterberg, D., Kaur, N., & Duckworth, O. W. (2017). Chemical speciation of potentially toxic trace metals in coal fly ash associated with the Kingston fly ash spill. *Energy & Fuels*, *31*(9), 9652-9659.

Saikia BK, Dutta AM, Saikia L et al (2014) Ultrasonic assisted cleaning of high sulphur Indian coals in water and mixed alkali. Fuel Processing Technology 123:107-113.

Santamarina, J. C., Torres-Cruz, L. A., & Bachus, R. C. (2019). Why coal ash and tailings dam disasters occur. *Science*, *364*(6440), 526-528.

Scala, F., & Clack, H. L. (2008). Mercury emissions from coal combustion: Modeling and comparison of Hg capture in a fabric filter versus an electrostatic precipitator. *Journal of hazardous materials*, *152*(2), 616-623.

Sebor, S. (2014). Environmental Strategies: Strategies for Compliance With Mercury and Air Toxics Standards. *Natural Gas & Electricity*, *31*(2), 8-13.

Seinfeld, J. H., & Pandis, S. N. (2016). *Atmospheric chemistry and physics: from air pollution to climate change*. John Wiley & Sons.

Teichmüller, M., & Teichmüller, R. (1966). Geological causes of coalification.

Tian L, Yang W, Chen Z et al (2016) Sulfur behavior during coal combustion in oxy-fuel circulating fluidized bed condition by using TG-FTIR. Journal of the Energy Institute 89:264-270.

Timpe RC, Mann MD, Pavlish JH, et al (2001) Organic sulfur and hap removal from coal using hydrothermal treatment. Fuel Processing Technology 73:127-141.

Uslu T, Atalay Ü (2004) Microwave heating of coal for enhanced magnetic removal of pyrite. Fuel Processing Technology 85:21-29.

Wang, Y. J., Duan, Y. F., Yang, L. G., Jiang, Y. M., Wu, C. J., Qian, W. A. N. G., & Yang, X. H. (2008). Comparison of mercury removal characteristic between fabric filter and electrostatic precipitators of coal-fired power plants. *Journal of Fuel Chemistry and Technology*, *36*(1), 23-29.

Wei, M., Zhao, X., Fu, L., & Zhang, S. (2017). Performance study and application of new coal-fired boiler flue gas heat recovery system. *Applied energy*, *188*, 121-129.

Weinhold, B. (2012). The future of fracking: new rules target air emissions for cleaner natural gas production.

Van Otten, B., Buitrago, P. A., Senior, C. L., & Silcox, G. D. (2011). Gas-phase oxidation of mercury by bromine and chlorine in flue gas. *Energy & Fuels*, *25*(8), 3530-3536.

Vasilakos NP, Corcoran WH (1983) Solvent effects in coal desulphurization by chlorinolysis near ambient temperature. Fuel 62:1111-1115.

Yan, R., Zhu, H., Zheng, C., & Xu, M. (2002). Emissions of organic hazardous air pollutants during Chinese coal combustion. *Energy*, *27*(5), 485-503.

Yan, R., Zheng, C., Wang, Y., & Zeng, Y. (2003). Evaluation of combustion characteristics of Chinese high-ash coals. *Energy & fuels*, *17*(6), 1522-1527.

Zhang L, Li Z, He W, et al (2018) Study on the change of organic sulfur forms in coal during low-temperature oxidation process. Fuel 222:350-361.

Zhao H, Lvov SN (2016) Phase behavior of the CO2–H2O system at temperatures of 273–623 K and pressures of 0.1–200 MPa using Peng-Robinson-Stryjek-Vera equation of state with a modified Wong-Sandler mixing rule: An extension to the CO2–CH4–H2O system. Fluid Phase Equilibria 417:96-108